Astronomy & Astrophysics manuscript no. paper2˙v6
January 19, 2013

RACE-OC Project: Rotation and variability in the ϵ Chamaeleontis, Octans, and Argus stellar associations ⋆ ⋆⋆

S. Messina[1], S. Desidera[2], A. C. Lanzafame[1,3], M. Turatto[1,4], and E. F. Guinan[5]

[1] INAF-Catania Astrophysical Observatory, via S.Sofia, 78 I-95123 Catania, Italy
e-mail: sergio.messina@oact.inaf.it
[2] INAF-Padova Astronomical Observatory, Vicolo dell'Osservatorio 5, I - 35122 Padova, Italy
e-mail: silvano.desidera@oapd.inaf.it
[3] University of Catania, Dept. of Physics and Astronomy, via S.Sofia, 78 I-95123 Catania, Italy
e-mail: alessandro.lanzafame@oact.inaf.it
[4] INAF-Trieste Astronomical Observatory, Via Tiepolo, 11 I - 34143 Trieste, Italy
e-mail: massimo.turatto@oats.inaf.it
[5] Dept. of Astronomy and Astrophysics, Villanova University, Villanova, 19085, PA, USA
e-mail: edward.guinan@villanova.edu

ABSTRACT

Context. Rotational properties of late-type low-mass members of associations of known age provide a fundamental source of information on stellar internal structure and its evolution.
Aims. We aim at determining the rotational and magnetic-related activity properties of stars at different stages of evolution. We focus our attention primarily on members of young stellar associations of known ages. Specifically, we extend our previous analysis in Paper I (Messina et al. 2010, A&A 520, A15) to 3 additional young stellar associations beyond 100 pc and with ages in the range 6-40 Myr: ϵ Chamaeleontis (∼6 Myr), Octans (∼20 Myr), and Argus (∼40 Myr). Additional rotational data of η Chamaeleontis and IC 2391 clusters are also considered.
Methods. Rotational periods were determined by applying the Lomb-Scargle periodogram technique to photometric time-series data obtained by the All Sky Automated Survey (ASAS) and the Wide Angle Search for Planets (SuperWASP) archives. The magnetic activity level was derived from the amplitude of the V light curves.
Results. We detected the rotational modulation and measured the rotation periods of 56 stars for the first time, confirmed 11 and revised 3 rotation periods already known from the literature. Adding the periods of 10 additional stars retrieved from the literature we determined a sample of 80 periodic stars at ages of ∼6, ∼20, and ∼40 Myr. Using the SuperWASP data we also revisited some of the targets studied in Paper I.
Conclusions. With the present study we have completed the analysis of the rotational properties of the late-type members of all known young loose associations in the solar neighbourhood. Considering also the results of Paper I, we have derived the rotation periods of 241 targets: 171 *confirmed,* 44 *likely*, 26 *uncertain.* The period of the remaining 50 stars known to be part of loose associations still remains unknown. The rotation period distributions we provided in the 0.8-1.2 $M_\odot$ mass range span nine different ages from 1 to ∼ 100 Myr. This rotation period catalogue, and specifically the new information presented in this paper at ∼6, 20, and 40 Myr, contributes significantly to a better observational description of the angular momentum evolution of young stars. The results of the angular momentum evolution model based on this period database will@ be presented in forthcoming papers.

Key words. Stars: activity - Stars: late-type - Stars: rotation - Stars: starspots - Stars: open clusters and associations: individual: ϵ Chamaeleontis association, η Chamaeleontis, Octans association, Argus association, IC 2391

1. Introduction

Rotation period measurements in open clusters and young associations provide a fundamental source of information on the angular momentum evolution of late-type stars. Stars in a cluster represent the most homogeneous sample (in age, initial chemical composition, and interstellar reddening) that can be empirically identified and are therefore essential for our understanding of stellar evolution. The identifications of young nearby stellar loose associations (e.g., Torres et al. 2008; Zuckerman & Song 2004, and references therein) have further extended the homogeneous stellar samples on which the early phases of stellar evolution can be investigated effectively. Nearby young associations are valuable targets for the characterisation of the stellar rotation and of the link with other stellar and environment properties. Like open clusters, in fact, physical association

Send offprint requests to: Sergio Messina

⋆ The online Tables B.2-B.5 and on-line Figs. **??-??** will be available in electronic form at the CDS via anonymous ftp to cdsarc.u-strasbg.fr (130.79.128.5) or via http://cdsweb.u-strasbg.fr/cgi-bin/qcat?J/A+A/

⋆⋆ Based on the All Sky Automated Survey (ASAS) and Wide Angle Search for Planets (SuperWASP) photometric data.

Table 1 Summary of the associations under study.

Association	Abbrev.	Age (Myr)	Distance (pc)	Known Members	Late-type Members	Periodic Members	Literature Period	New Period (+Revised)
ϵ / η Chamaeleontis	ϵ / η Cha	6	108	41	30	14(25)	9	10 (+2)
Octans	Oct	20?	141	15	12	8(10)	0	9 (+0)
Argus / IC 2391	Arg / IC 2391	40	106	65	57	23(45)	1	37 (+1)

allows us to study ensembles of stars with similar age and native environment and reduce the uncertainties due to intrinsic dispersion (still of unknown origin) of rotation period, light elements abundance, and magnetic activity. Such systems are targets of several dedicated studies like spectral characterisation and searches for planets and circumstellar discs (e.g. Torres et al. 2006; Setiawan et al. 2008; Chauvin et al. 2010; Carpenter et al. 2009).

In recent years, a number of valuable monitoring projects of young and intermediate-age open clusters (see, e.g., Herbst & Mundt 2005; Herbst et al. 2007; Hodgkin et al. 2006; von Braun et al. 2005) have provided enough data for statistical analyses of the rotational evolution of solar-like stars. Irwin & Bouvier (2009) report a compilation of 3100 period measurements available then. More recent measures of photometric rotation periods include those of 575 stars in M37 by Hartman et al. (2009), 368 Pleiades stars by Hartman et al. (2010), 122 stars in M37 by Messina et al. (2008), 38 stars in M11 by Messina et al. (2010a), 46 stars in Coma Berenicis by Collier Cameron et al. (2009), and 55 stars in M34 by James et al. (2010). Extensive survey work in clusters at 1-2 Myr, mainly the Orion Nebula Cluster (ONC) and NGC 2264, have established the initial distribution of rotation rates in low-mass stars (Stassun et al. 1999; Herbst et al. 2001; Rebull 2001; Makidon et al. 2004; Lamm et al. 2004). Herbst & Mundt (2005) estimate that 50-60% of the stars on convective tracks are released from any locking mechanisms very early on and spin-up as a consequence of their contraction in the pre-main sequence (PMS), and these stars account for the rapidly rotating young main sequence stars. The other 40-50% lose substantial amounts of angular momentum during the first few million years, and end up as slowly rotating main sequence stars. The duration of the rapid angular momentum loss phase is ∼5-6 Myr, which is roughly consistent with the lifetime of discs estimated from infrared surveys of young clusters. This supports the hypothesis that the interaction with a circumstellar disc drains angular momentum from the star, thus delaying its spin up for the (variable) duration of its lifetime (e.g., Haisch et al. 2001). This process is not understood in detail yet (see, e.g., Collier Cameron & Campbell 1993; Shu et al. 1994; Matt et al. 2010) and is usually modelled by means of very simplified assumptions, e.g., the disc-locking hypothesis (Köenigl 1991; Collier Cameron et al. 1995) or accretion-driven stellar wind (e.g., Matt & Pudritz 1995).

The initial distribution of rotation rates and the strong rotational regulation in the first ∼5Myr are deemed responsible for the dispersion of rotation periods at a given mass seen in individual young clusters from the PMS until the age of the Hyades. For the Hyades, a narrow correlation between the B−V colours and the rotation periods of F, G, and K stars has been found (Radick et al. 1987). A small scatter of the individual stellar rotation rates about the mean period-colour relation has also been found on M37 (Messina et al. 2008; Hartman et al. 2009), M35 (Meibom, Mathieu, & Stassun 2009), and Coma Berenicess (Collier Cameron et al. 2009). The convergence of the spin rates in ∼600 Myr is a consequence of the strong dependence on stellar rotation rate of the angular momentum loss via a thermally driven magnetically channelled wind (e.g., Mestel & Spruit 1987; see also Weber & Davis 1967; Kawaler 1988; Chaboyer et al. 1995a,b). For such a convergence to occur at the age of the Hyades, the timescale for coupling the stars radiative interior to its outer convective zone must also be significantly shorter than the Hyades age (see, e.g., Collier Cameron et al. 2009).

The relationship between age, rotation, and activity has been a crucial topic of stellar evolution over the past 40 years. Angular momentum loss due to stellar winds is generally thought to be responsible for the Skumanich (1972) law, but the exact dependence of rotational velocity on age is not entirely clear, and it relies on the assumed stellar magnetic field geometry and degree of core-envelope coupling (Kawaler 1988; Krishnamurthi et al. 1997). Empirical age-rotation relations have been proposed to determine the age of stars, a method referred to as gyrochronology (e.g., Barnes 2003, 2007; Mamajek & Hillenbrand 2008; Collier Cameron et al. 2009; Barnes 2010). Empirical age-activity relations have also been proposed, though these do not always find activity decaying with time quite as simply as predicted by the Skumanich law (e.g., Feigelson et al. 2004; Pace & Pasquini 2004; Giampapa et al. 2006).

The determination of stellar rotational periods in large samples of stars of different ages and mass is also crucial for understanding the relationships with stellar properties and their close surroundings. It is also expected that the dissipation timescale of circumstellar discs is related to the processes of planets formation (e.g. Bouvier 2008). On the other hand, the presence of planets may in turn influence the stellar rotational evolution. Recently, Pont (2009) has investigated the influence of tidal interaction with close-in giant planets (Hot Jupiters), and Lanza (2010) studied the role of Hot Jupiter interaction with the coronal magnetic field in the stellar angular momentum loss rate via a magnetised wind.

Open clusters also represent a unique testbed for studying the Li depletion with age and its relationships with stellar rotation (e.g., Sestito & Randich 2005, Jeffries & Oliveira 2005, Randich et al. 2005). In fact, stellar rotation plays a role in shaping the internal circulation, which in turn affects the abundance of light elements that are easily destroyed in the stellar interior (Li, Be, B). A survey of Li abundances in young stellar associations has been carried out by da Silva et al. (2009), who also studied the relationships with age and $v \sin i$.

While significant progress has been attained in the last few years, thanks to several dedicated projects or as a by-product of high-precision photometric planet-transit surveys, our knowledge of the rotation evolution of late-type stars remains incomplete, so firm confirmation of the correlations proposed above is still needed. RACE-OC (Rotation

and ACtivity Evolution in Open Clusters) is a long-term project designed to study the evolution of the rotational properties and the magnetic activity of late-type members of stellar open clusters with ages between 1 to about 600 Myr (Messina 2007; Messina et al. 2008, 2010a). In Messina et al. (2010b, hereafter Paper I), we considered stellar associations at distances closer than 100 pc and ages younger than about 100 Myr from the list of Torres et al. (2008). These are TW Hydrae, β Pictoris, Tucana/Horologium, Columba, Carina, and AB Doradus associations. They span ages between 8 and 100 Myr and, therefore, allow us to study the angular momentum evolution close to the crucial phase of dissipation of circumstellar discs and planet formation. In Paper I, we determined rotational periods for 144 of 204 late-type members of these associations. A clear indication of evolution with time of rotational period and of its photometric signatures (e.g., photometric amplitude of light curve) has been observed. The goal of the present paper is to complete the study of the associations identified by Torres et al. (2008), determining the rotational properties of members of ϵ Chamaeleontis, Octans, and Argus associations ($\sim$6, 20, and 40 Myr, respectively), with mean distances between 110 and 150 pc.

In Sect.2, we present the sample considered in the present study. In Sect. 3, we describe the photometric data that are used in our analysis. In Sect. 4, we describe our procedure for the rotation period search. In Sect. 5, we present our results. Conclusions are given in Sect. 6. In the Appendix we present the results on periods for a few revisited targets in Paper I.

2. The sample

The sample of our investigation is taken from the compilation of Torres et al. (2008), which includes an updated analysis of the membership of nearby associations younger than 100 Myr. We selected the following associations that have mean distances beyond 100 pc: ϵ Chamaeleontis, Octans, and Argus. These associations are reported with ages in the range $\sim$6 to $\sim$40 Myr (cfr. Table 1).

The ϵ Chamaeleontis association was discovered and characterised by Frink et al. (1998). We selected 15 late-type members: 14 are high-probability members from the compilation of Torres et al. (2008) and one is a recently added member by Kiss et al. (2011) as part of the RAVE (Radial Velocity Experiment) project. Given the possible connection with ϵ Chamaeleontis, as first suggested by Mamajek et al. (1999), we also compiled a list of all (15) late-type members of the η Chamaeleontis cluster from Torres et al. (2008), whose age is estimated as around 4-9 Myr. Four cluster members with good kinematic data were found as high-probability members of the ϵ Cha association. In the following analysis we consider both η and ϵ Cha members as coeval with an age of $\sim$ 6 Myr, but we continue to use different symbols to distinguish them.

The Octans association was discovered within the SACY project (Torres et al. 2003). Owing to its mean distance of about 140 pc and the small number of members with trigonometric parallax, the accuracies on distance of individual members and age ($\sim$ 20 Myr) are poorer than for other associations found with the same approach and the discovered members mostly have G spectral type. Torres et al. (2008) give an updated list of members of this association from which we selected a sample of 12 members with spectral type later than F.

The Argus association was also discovered by Torres et al. (2003) in the SACY survey. Based on the convergence method and following the suggestion of Makarov & Urban (2000), they found that the kinematic properties of the members of the IC 2391 open cluster are in good agreement with their proposed Argus members. Torres et al. (2008) give an updated list of members of both Argus and IC 2391 members. Finally, we also considered the new candidates members of young associations recently identified by Kiss et al. (2011) from RAVE data and by Desidera et al. (2011). From these lists, we compiled a sample of 57 members (27 Argus stars and 30 stars in IC 2391) with spectral type later than F.

From the initial list of 121 known stellar members, we selected 99 late-type stars (spectral types later than F or colours consistent with a late spectral type) that are suitable for the photometric search of rotational modulations. In Table 1 we list name, abbreviation, age, and mean distance of the associations under study (Torres et al. 2008), together with the number of known members and late-type members selected for period search. Most of the spectroscopic information (spectral types, projected rotational velocity $v \sin i$) is from SACY database (Torres et al. 2006). In the case of IC 2391 cluster, $v \sin i$ values come from da Silva et al. (2009) and Marsden et al. (2009). Additional bibliography for individual targets is given in Appendix A.

Furthermore, to complete the analysis of the associations studied in Paper I, we considered the photometry becoming available in the Wide Angle Search for Planets (SuperWASP) archive for the stars of TW Hydrae, β Pictoris, Tucana/Horologium, Columba, Carina and AB Doradus associations. The new rotation periods of the associations studied in Paper I and retrieved from SuperWASP photometry are reported in Appendix B.

3. Data

3.1. The ASAS photometry

As in Paper I, most of the present analysis is based on data from the All Sky Automated Survey (ASAS) (Pojmanski 1997; 2002). The ASAS project is monitoring all stars brighter than V=14 at declinations $\delta < +28^\circ$, with typical sampling of 2 days. The ASAS archive[1] ensures long-term monitoring since it contains data from 1997 to date. A short-term monitoring might hamper the identification of the correct rotational period. Since the configuration of active regions, which is responsible for the light rotational modulation, evolves with time, such a long time-span is particularly suitable for our purposes.

The linear scale at focal plane is 16 arcsec/pixel. The FWHM of stellar images is 1.3-1.8 pixels. Aperture photometry through five apertures is available in the ASAS catalogue. The choice of the aperture adopted in our analysis was made star by star by selecting the aperture giving the highest photometric precision (i.e., the minimum average magnitude uncertainty).

[1] www.astrouw.edu.pl/asas/

Table 2 ϵ **Cha association and** η **Cha cluster**: summary of period searches.

Name	ID_{ASAS}	P (d)	ΔP (d)	Timeseries Sections	Qual. Flag	ΔV_{max} (mag)	σ_{acc} (mag)	V_{min} (mag)	B−V (mag)	Sp.T.	Note	Variable's Name
					ϵ Chamaeleontis							
CP-68 1388	105749-6914.0	3.560	0.030	12(13)/15	C	0.25	0.03	10.38	0.86^{Av}	K1V(e)	new	
GSC 9419-01065	114932-7851.0	8.000^{c}	0.100	4(10)/12	U	0.37	0.03	12.61	1.27^{Av}	M0Ve	new	DZ Cha
HIP 58285	115715-7921.5	...	...	...	...	...	...	12.0	0.93^{d}	K0e	...	T Cha
HIP 58490	115942-7601.4	8.000	0.100	7(11)/13	C	0.20	0.03	11.02	1.11^{Av}	K4Ve	new	
HD 104237E	120005-7811.6	2.45	...	1/1	U	...	...	12.08	1.11^{d}	K4Ve	B; P_{lit}	
HD 104467	120139-7859.3	4.430	0.040	4(8)/13	L	0.05	0.03	8.45	0.63^{Av}	G3V(e)	new	
GSC 9420-0948	120204-7853.1	4.450	0.040	11(13)/13	C	0.48	0.03	12.30	1.00^{Av}	M0e	new	
GSC 9416-1029	120437-7731.6	5.350	...	1/1	U	...	...	13.81	1.30^{Av}	M2e	SB2; P_{lit}	
HD 105923	121138-7110.6	5.050	0.050	11(13)/14	C	0.07	0.03	9.07	0.73^{Av}	G8V	new	
GSC 9239-1495	121944-7403.9	...	...	...	...	...	...	12.54	1.28^{Av}	M0e	...	
GSC 9239-1572	122023-7407.7	1.536	0.002	9(8)/9	C	0.30	0.03	12.85	0.97^{Av}	M1V	V; new	
CD-74 712	123921-7502.7	3.970	0.030	23(24)/25	C	0.13	0.03	10.22	0.97	K3Ve	new	
GSC 9235-1702	122105-7116.9	6.85	0.05	9(14)/14	C	0.25	0.02	11.62	1.20^{d}	K7V	P=P_{lit}	
CD-69 1055	125826-7028.8	2.007	0.007	8(13)/15	C	0.10	0.03	9.91	0.83^{Av}	K0Ve	new	
TYC 9246-971-1	132208-6938.2	3.750	0.030	9(14)/15	C	0.13	0.03	10.31	0.86^{Av}	K1Ve	new	MP Mus
					η Chamaeleontis cluster							
RECX 1	083656-7856.8	4.50	0.040	12(12)/15	C	0.13	0.03	10.36	1.19	K4V	V; P=2P_{lit}	EG Cha
RECX 3^{a}	084136-7903.7	3.57	...	2/2	U	0.08	...	14.30	...	M3	P_{lit}	EH Cha
RECX 4	084229-7903.9	7.1	0.4	6(10)/12	C	0.25	0.03	12.73	...	K7	P=P_{lit}	EI Cha
RECX 5	084235-7858.1	3.11	...	1/2	U	0.03	...	15.17	...	M5	P_{lit}	EK Cha
RECX 6^{a}	084239-7854.7	1.84	...	2/2	U	0.16	...	13.98	...	M7	P_{lit}	EL Cha
RECX 7^{a}	084302-7904.7	2.62	...	2/2	U	0.09	...	10.76	...	M3	SB2; P_{lit}	EM Cha
RECX 9^{a}	084419-7859.1	1.71	...	2/2	U	0.38	...	14.75	...	M4	V; P_{lit}	EN Cha
RECX 10	084432-7846.6	20.0	3.0	5(5)/12	C	0.26	0.03	12.41	...	K7	P=P_{lit}	EO Cha
RECX 11	084708-7859.6	4.84	0.04	7(7)/12	C	0.28	0.03	11.00	...	K4	P≠P_{lit}	EP Cha
RECX 12	084802-7855.0	1.26^{b}	0.05	2(2)/12	C	0.18	0.03	13.92	0.73	M3e	V; P= P_{lit}	EQ Cha
RECX 14	...	1.73	...	2/2	U	0.04	...	17.07	...	M5e	P_{lit}	ES Cha
RECX 15^{a}	084319-7905.4	12.8	...	2/2	U	0.44	...	13.97	...	M3e	P_{lit}	ET Cha
RECX 16	.....	...	...	...	....	...	...	17.07	...	M5e	...	
RECX 17	.....	...	...	...	....	...	...	16.82	...	M5e	...	
RECX 18	.....	...	...	...	....	...	...	17.66	...	M5e	...	

V=visual companion; B=binary system; P_{lit}: period as given in the literature; [a]: ASAS very sparse observations;
[b]: period undetected in the periodogram of the complete time series; [c]: $v \sin i$ inconsistent with $v_{eq}=2\pi R/P$;
[d]: from Sp. type; ^{Av}: V mag and B−V corrected for reddening.

Table 3 As in Table 2 for **Octans Association**.

Name	ID_{ASAS}	P (d)	ΔP (d)	Timeseries Sections	Qual. Flag	ΔV_{max} (mag)	σ_{acc} (mag)	V_{min} (mag)	B−V (mag)	Sp.T.	Note	Variable's Name
CD-58 860	041156-5801.8	1.612	0.005	9(10)/12	C	0.10	0.03	9.92	0.68	G6V	new	
CD-43 1451	043027-4248.8	...	...	...	...	...	...	10.75	0.79	G9V(e)	...	
CD-72 248	050651-7221.2	0.236	0.001	6(6)/12	C	0.09	0.03	10.70	0.82	K0I	new	
HD 274576	052851-4628.3	2.220	0.020	9(10)/12	C	0.10	0.03	10.48	0.66	G6V	new	
CD-47 1999	054332-4741.2	1.265	0.004	3(6)/12	C	0.08	0.03	10.05	0.56	G9V(e)	P=P_{ACVS}	
TYC 7066-1037-1	055812-3500.8	2.470^{b}	0.040	6(9)/14	C	0.08	0.03	11.14	0.80^{Av}	G9V	new	
CD-66 395	062515-6629.5	0.371	0.001	6(10)/12	C	0.16	0.03	10.75	0.71	K0I	new	
TYC 9300-0529-1	184949-7157.2	2.550^{b}	0.030	4(14)/14	L	0.06	0.03	11.59	0.80	K0V	V; new	
TYC 9300-0891-1	184949-7157.2	...	...	...	...	...	...	11.43	0.77	K0V(e)	V	
CP-79 1037	194704-7857.7	1.950^{b}	0.020	5(6)/13	C	0.05	0.03	11.18	0.75	G8V	new	
CP-82 784	195357-8240.7	1.373	0.003	9(9)/13	C	0.08	0.03	10.81	0.85	K1V	new	
CD-87 121	235818-8626.4	0.762	0.002	4(6)/12	L	0.03	0.03	9.94	0.74	G8V	V?; new	

V=visual companion; P_{ACVS}: period in ACVS; [b]: period undetected in the periodogram of the complete time series;
^{Av}: V mag and B−V corrected for reddening.

3.2. The SuperWASP photometry

The SuperWASP project (Pollacco et al. 2006) recently released the first public data archive (Butters et al. 2010) [2]. Light curves from 2004 to 2008 for both the northern and southern observatories are included. Temporal and spatial coverage is irregular, but extended enough to make a systematic search for photometric timeseries of our targets meaningful. The observing procedure includes sequences up to nine hours long for stars at the most favourable sky declinations with a sampling of about ten minutes. The SuperWASP data have therefore a better sensitivity to periods $\lesssim 1$ d than the ASAS data. We then checked the availability in SuperWASP archive of data for both the targets studied in this paper as well those we studied in Paper I. To further complete Paper I analysis, we also checked the availability of ASAS and SuperWASP photometry for the new candidates members of young MG identified by Kiss et al. (2011). Our analysis is based on the processed flux measurements obtained through application of the SYSREM algorithm (Tamuz et al. 2005). SuperWASP observations were collected in 2004 without any light filter, the spectral transmission defined by the optics, detector, and atmosphere. Starting from 2006 they were collected through a wide band filter in the 400-700 nm. Owing to differences

[2] www.wasp.le.ac.uk/public/

Table 4 As in Table 2 for **Argus Association and IC 2391 cluster**.

Name	ID_{ASAS}	P (d)	ΔP (d)	Timeseries Sections	Qual. Flag	ΔV_{max} (mag)	σ_{acc} (mag)	V_{min} (mag)	B−V (mag)	Sp.T.	Note	Variable's Name
				Argus								
HD 5578	005655-5152.5	1.461	0.005	4(5)/6	L	0.05	0.03	9.62	0.99	K3V	V; new	BW Phe
CD-49 1902	054945-4918.4	1.100	0.005	3(6)/8	L	0.09	0.03	11.30	0.69	G7V	new	
CD-56 1438	054945-4918.4	0.240	0.002	1(4)/8	U	0.08	0.03	11.10	0.66	K0V	new	
CD-28 3434	064945-2859.3	3.820	0.030	7(7)/10	C	0.06	0.03	10.38	0.75[a]	G7V	new	
CD-42 2906	070153-4227.9	3.950	0.060	4(6)/7	L	0.09	0.03	10.50	0.84	K1V	new	
CD-48 2972	072822-4908.6	1.038	0.004	6(3)/8	C	0.11	0.03	9.78	0.80	G8V	P≠P_{ACVS}	
HD 61005	073547-3212.2	5.04	0.03	3(10)/14	C	0.05	0.03	8.19	0.75	G8V	new	
CD-48 3199	074726-4902.9	2.190	0.010	6(5)/7	C	0.06	0.03	10.40	0.65	G7V	new	
CD-43 3604	074851-4327.3	0.890	0.001	4(6)/9	L	0.10	0.03	10.88	0.92	K4V	new	
TYC 8561-0970-1	075355-5710.1	...	...	...	...	0.00	0.00	11.50	0.83[Av]	K0V	...	
CD-58 2194	083912-5834.5	5.160[c]	0.040	3(4)/7	U	0.04	0.03	10.08	0.62	G5V	new	
CD-57 2315	085008-5746.0	...	...	...	...	...	...	10.21	0.83	K3V	...	
TYC 8594-0058-1	090204-5808.8	0.982	0.002	4(4)/7	U	0.05	0.03	11.08	0.71	G8V	new	
CPD-62 1197	091330-6259.2	1.260[c]	0.001	7(5)/9	U	0.05	0.03	10.46	0.81	K0V	new	
TYC 7695-0335-1	092854-4101.3	0.391	0.001	7(7)/9	C	0.10	0.03	11.62	0.67	K3V	new	
HD 84075	093618-7820.7	...	...	...	...	...	...	8.59	0.59	G1	...	
TYC 9217-0641-1	094247-7239.8	2.300	0.010	6(6)/8	C	0.16	0.03	12.18	0.65	K1V	new	
CD-39 5883	094718-4002.9	4.060[b]	0.030	5(5)/9	C	0.04	0.03	10.74	0.81[a]	K0V	new	
HD 85151A	094843-4454.1	0.970	0.005	5(5)/5	C	0.02	0.01	9.10	0.50	G7V	V; new	
CD-65 817	094909-6540.3	2.740	0.020	4(4)/7	U	0.04	0.03	10.33	0.63	G5V	V; new	
HD 309851	095558-6721.4	1.816	0.007	5(5)/7	C	0.06	0.03	9.78	0.60	G1V	new	
HD 310316	104956-6951.4	3.610	0.030	4(6)/9	L	0.06	0.03	10.82	0.73	G8V	V; new	
CP-69 1432	105351-7002.3	1.030	0.002	3(5)/8	L	0.06	0.03	10.66	0.62	G2V	new	
CD-74 673	122034-7539.5	3.480	0.020	6(6)/8	C	0.07	0.03	10.49	1.02	K3V	SB; new	
CD-75 652	134913-7549.8	2.270	0.010	9(8)/9	C	0.08	0.03	9.61	0.68	G1V	new	
HD 133813	151223-7515.3	4.090	0.030	8(7)/10	C	0.07	0.03	9.27	0.84	G9V	new	NY Aps
CD-52 9381	200724-5147.5	0.830	0.001	5(6)/9	C	0.12	0.03	10.53	1.24	K6V	P=P_{ACVS}	
				IC 2391								
PMM 7422 TYC 8162-1020-1	082844-5205.7	1.512	0.005	7(6)/9	C	0.11	0.03	10.40	0.69	G6	new	
PMM 7956 1RXS J082952.7-514030	082952-5140.7	...	...	...	...	0.00	0.00	11.50	0.97	K2e	...	
PMM 1560 TYC 8568-1413-1	082952-5322.0	...	...	...	...	0.00	0.00	10.64	0.61	G3	...	
PMM 6974 TYC 8162-754-1	083418-5216.0	7.800	0.050	4(3)/8	U	0.10	0.03	12.04	1.04	...	new	
PMM 4280 TYC 8568-407-1	083421-5250.1	...	...	...	...	0.00	0.00	10.04	0.67	G5	...	
PMM 6978 1RXS J083502.7-521339	083501-5214.0	5.100	0.200	4(5)/8	L	0.11	0.03	12.01	1.02	...	new	
PMM 2456 1RXS J083543.4-532123	083544-5321.3	...	...	...	...	0.00	0.00	12.16	0.92	K3e	...	
PMM 351 1RXS J083624.5-540101	083624-5401.1	1.923[c]	0.007	6(4)/7	U	0.06	0.03	10.17	0.57	G0	new	
PMM 3359	083655-5308.5	3.840	0.030	6(3)/8	C	0.05	0.03	11.38	0.76	...	new	
PMM 5376	083703-5247.0	...	...	...	...	0.00	0.00	13.94	1.37	Me	...	
PMM665 2MASS J08375156-5345458	083752-5345.8	4.510	0.040	3(4)/8	U	0.07	0.03	11.33	0.75	G8	new	
PMM 4336 VXR PSPC 2a	083756-5257.1	3.71	0.03	4(5)/9	L	0.06	0.03	11.25	0.86	G9	new	
PMM 4362 CD-52 2467	083823-5256.8	3.930	0.030	4(4)/9	U	0.05	0.03	10.91	0.67	...	new	VXR 3a
PMM 4413 CD-52 2472	083856-5257.9	5.05	0.05	3(2)/9	U	0.03	0.03	10.20	0.67	G2	SB2, new	VXR 5
PMM 686 1RXS J083921.9-535420	083923-5355.1	4.410	0.050	2(0)/7	U	0.05	0.03	12.55	1.04	K4e	new	
PMM 4467 VXR PSPC 12	083953-5257.9	3.850	0.030	7(7)/9	C	0.17	0.03	11.84	0.84	K0(e	P=P_{lit}	V364 Vel
PMM 1083 VXR PSPC 14	084006-5338.1	1.333	0.004	8(8)/8	C	0.07	0.03	10.38	0.57	G0	P=P_{lit}	V365 Vel
PMM 8415 VXR PSPC 16a	084016-5256.5	...	...	...	...	0.00	0.00	11.63	0.87	G9(e)	...	
PMM 1759 VXR PSPC 18	084018-5330.4	...	...	...	...	0.00	0.00	12.54	1.01[Av]	K3e	...	
PMM 1142 VXR PSPC 22a	084049-5337.8	...	...	...	...	0.00	0.00	11.04	0.68	G6	...	
PMM 1820 VXR PSPC 35a	084126-5322.7	0.527[b]	0.001	4(5)/8	C	0.12	0.03	12.41	1.00	K3e	P=P_{lit}	V366 Vel
PMM 4636 VXR PSPC 41	084158-5252.2	...	...	...	...	0.00	0.00	13.20	1.26	K7e	...	V368 Vel
PMM 3695 VXR PSPC 47	084219-5301.9	0.223	...	...	U	0.00	0.00	13.60	1.44	M2e	P_{lit}	V371 Vel
PMM 756	084300-5354.1	3.140	0.020	7(7)/7	C	0.13	0.03	11.06	0.68	G9	new	
PMM 2012 VXR PSPC 69	084359-5333.7	2.210	0.010	4(4)/8	U	0.10	0.03	11.41	0.83	K0(e)	new	
PMM 4809 VXR PSPC 70	084405-5253.3	2.600	0.010	6(7)/9	C	0.08	0.03	10.73	0.64	G3(e)	new	V376 Vel
PMM 1373	084410-5343.6	5.380	0.060	1(2)/8	U	0.06	0.03	12.06	0.96	...	new	
PMM 5884 VXR PSPC 72	084426-5242.5	3.030	0.020	5(6)/9	C	0.07	0.03	11.35	0.73	G9(e)	P=P_{lit}	V377 Vel
PMM 4902 VXR PSPC 76a	084526-5252.0	4.820[b]	0.050	4(2)/9	C	0.10	0.03	12.45	1.05	K3e	P=P_{lit}	V379 Vel
PMM 2182 TYC 8569-2769-1	084548-5325.8	1.437[b]	0.002	8(4)/8	C	0.06	0.03	10.18	0.63	G2(e)	new	

V=visual companion; SB=binary system; P_{lit}: period as given in the literature; P_{ACVS}: period in ACVS;
[b]: period undetected in the periodogram of the complete time series; [c]: $v \sin i$ inconsistent with $v_{eq}=2\pi R/P$;
[Av]: V mag and B−V corrected for reddening.

in spectral bands with respect to the standard Johnson V ASAS data, we decided to analyse the SuperWASP data independently without merging these with ASAS data.

3.3. Data from the literature

Literature period determinations, including those listed in ASAS Catalogue of Variable Stars (ACVS) and the search for variable stars from SuperWASP data (Norton et al. 2007), were considered and compared to our measurements when available. These are listed in Tables 2-4. Three cases of discrepant results are discussed individually in Appendix A.

4. Photometry rotation period search

The rotational period search procedure is described in Paper I. Here we briefly summarise it. The analysis makes

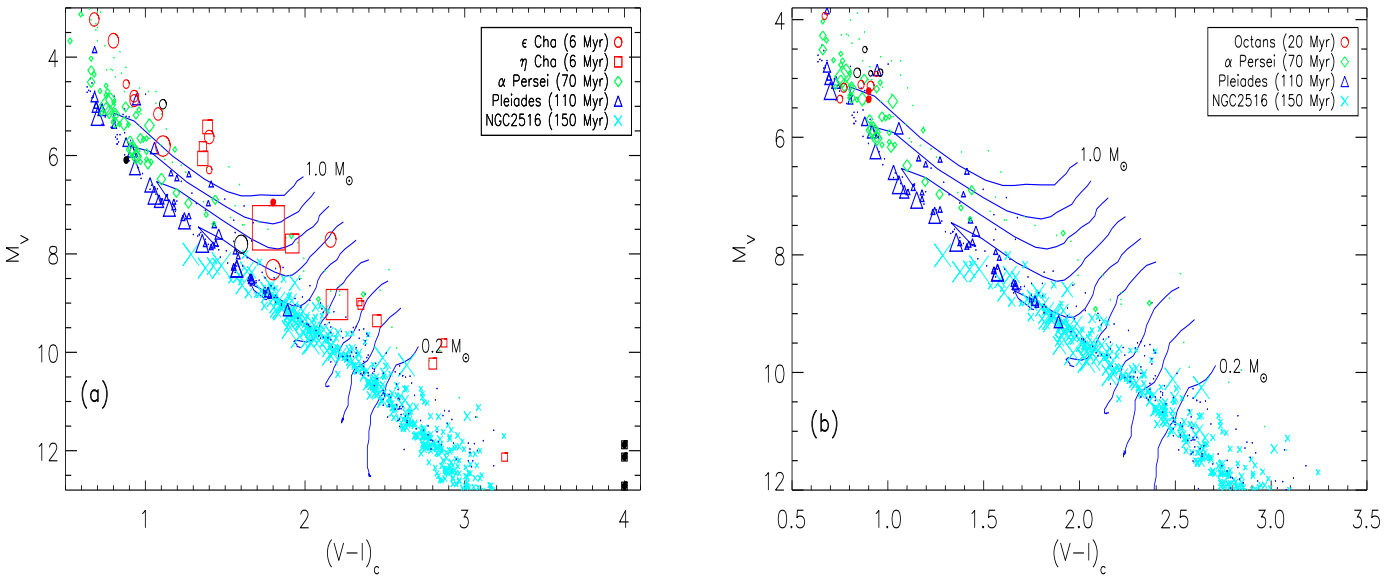

Fig. 1 Colour-corrected colour-magnitude diagrams with overplotted PMS tracks (solid lines) from Baraffe et al. (1998) for ϵ and η Cha (left) and Octans (right). Different symbols indicate stars belonging to different association/clusters; bigger symbols indicate longer rotation periods. Filled symbols represent members with unknown rotation period. Black symbols represent stars whose V−I colour is derived from spectral type.

use of the Lomb-Scargle periodogram (Scargle 1982). The light curves of late-type active stars are typically characterised by changes in amplitude and shape with timescales of a few months or even shorter (see, e.g., Messina et al. 2004). These are due to the finite lifetime of active regions, consisting of either dark spots or bright faculae, and to differential rotation. Additional photometric variability is observed on timescales shorter and longer than the rotation period because of flares and magnetic cycles. This variability pattern causes the application of the Lomb-Scargle periodogram to the whole light curve to fail the detection of the rotational period in some cases. Therefore, in addition to analysing the whole timeseries (which is typically 8-yr long for ASAS data and 4-yr long for SuperWASP data), we performed the period search on light-curve segments not exceeding two months.

The determination of the false alarm probability (FAP) is a crucial issue for evaluating the significance of detected periodicities. The existence of significant correlations between data that are collected on shorter timescales than the stellar variability does not allow safely making the assumption that each observed data point is independent of the others (Herbst & Wittenmyer 1996; Stassun et al. 1999; Rebull 2001; Lamm et al. 2004). To overcome this difficulty, we follow the bootstrap approach proposed by Herbst et al. (2002). For each light curve segment, we scramble 1000 times the day numbers of the Julian Day (JD) while keeping photometric magnitudes and the decimal part of the JD unchanged. Then we perform the period search on each fake randomised dataset, comparing the power of the highest peak to that observed on the real dataset to obtain the FAP. We adopt a confidence level larger than 99% (FAP<0.01) as detection threshold for a significant detection.

Finally, to successfully identify the true rotational periodicity, it is necessary to consider aliases, which might have even higher power than the true period. The spectral window function is inspected to disentangle aliases (1-d peak, beat periods between the star's rotation period (P) and the data sampling). The uncertainties in the period determination were derived following Lamm et al. (2004).

For each target we report (Tables 2-4) the detected rotation period, together with the number of segments in which such a period was derived, with a confidence level higher than 99%. In some cases, however, the same period was found in other segments with a confidence level below 99%, but the lightcurve still showed a clear rotational modulation with this very period. We therefore also report the number of segments in which the lightcurve, when phased with the detected rotation period, shows a smooth sinusoidal variation; in this case, the average residual in the sinusoidal fit of the light curve is smaller than the light-curve amplitude. The number of segments in which the period was found with a confidence level higher than 99% and/or the number of segments in which the phased lightcurve show average residuals lower than its amplitude can be used to estimate the robustness of the period determination. When $v \sin i$ measurements are also available, a consistency check can be performed with the equatorial velocity, which can be derived from the rotational period and an estimate of the stellar radius. We use this information to classify the detected periods according to their reliability.

Periods derived in at least five segments, or in less than five but with an independent confirmation from the literature, and that are consistent with $v \sin i$ will be referred to as *confirmed* periods (C). Periods derived in less than five segments that are consistent with $v \sin i$ and that produce mean residuals in the sinusoidal fit less than the light-curve amplitude in at least five segments will be referred to as *likely* periods (L). Periods derived in less than five segments that produce mean residuals in the sinusoidal fit less

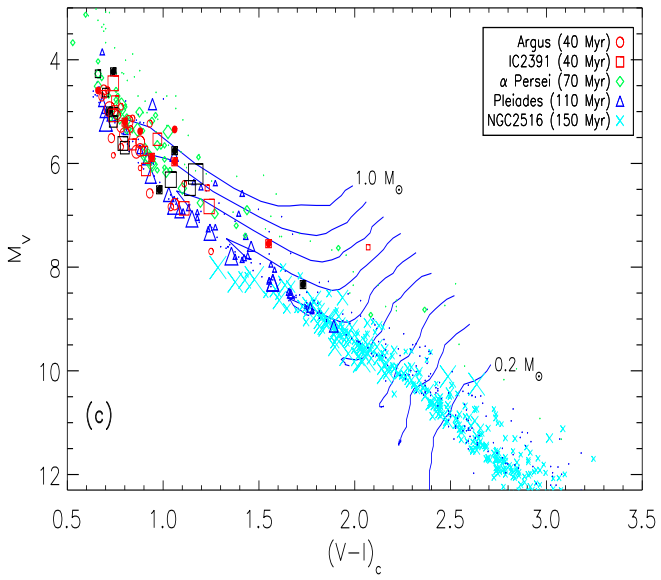

Fig. 2 As in Fig. 1 for Argus and IC 2391.

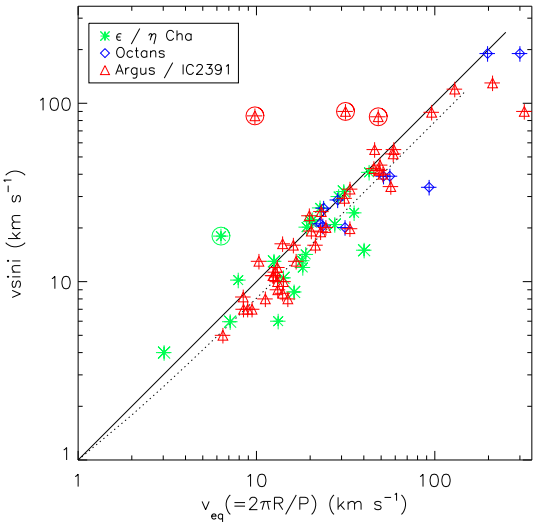

Fig. 3 $v \sin i$ from the literature vs. equatorial velocity v_{eq} = $2\pi R/P$. The solid line marks $v \sin i = v_{eq}$, whereas the dotted line $v \sin i = (\pi/4) v_{eq}$. Circled symbols are stars whose $v \sin i$ is inconsistent with v_{eq}.

Table 5 Summary of results of the comparison between $v \sin i$ and equatorial velocity.

Association	# Stars	$<\sin i> \pm \sigma$	r	Significance Level
ϵ Cha	10	0.85±0.22	0.89	a
η Cha	8	0.80±0.25	0.61	b
ϵ/η Cha	18	0.83±0.22	0.76	a
Octans	10	0.79±0.22	0.94	a
Argus	17	0.86±0.23	0.96	a
IC2391	19	0.76±0.22	0.82	a
Arg / IC2391	36	0.81±0.16	0.84	a

a: confidence level > 99.999%; b: confidence level = 99.995%.

than the light-curve amplitude in less than five segments, or with only 1-2 determinations in the literatures, or that are inconsistent with $v \sin i$ will be referred to as *uncertain* periods (U).

5. Results

The results of our investigation are summarised in Table 1, where we report the total number of *confirmed* periodic members (and the total number of *confirmed* + *likely* + *uncertain* in paretheses), the number of periodic members with period adopted from the literature, new periods determined from this study (and periods revised by us with respect to earlier literature values).

We determined 45 *confirmed* rotation periods (31 of which are new determinations), 11 *likely*, 24 *uncertain* (10 of which are taken from the literature). Eleven of 80 periodic stars were already known from the literature and we could confirm their rotation period, whereas we revised it for 3 stars (RECX 1, RECX 11, and CD-48 2972, see Appendix A). The rotation periods of 19 stars remain unknown, for three of which we have data neither in ASAS, in SuperWasp, nor in the literature, whereas for 16 we find non-periodic variability. In Tables 2-4 we report the results of a period search in some detail for the members of individual associations. As in Paper I, the results of the period search for close spectroscopic binaries whose rotation might be altered by the tides of their companions is here reported. However, they are excluded from the rotational distributions and also when computing the mean and median values in the subsequent sections. In the online Table B.2, we list the rotation periods for each periodic target, together with uncertainties and normalised powers, determined in the individual time-series segments.

The light curves of all stars for which either the ASAS or the SuperWASP photometry allowed us to determine the rotation period are plotted in the online Figs. **??-??**.

5.1. Colour-magnitude diagrams

Following the approach of Paper I, we use the M_V vs. V−I CMD and a set of low-mass PMS evolutionary tracks to derive masses and radii. Owing to the targets distances, on average larger than 100 pc, and their young ages, especially in the case of the ϵ / η Cha members, the observed colours may suffer from reddening arising either from interstellar or circumstellar material. We have investigated on the possible colour excess of all targets and derived the intrinsic colours for the subsequent analysis. V magnitudes are taken from ASAS because the long-term monitoring gives the possibility of measuring the brightest magnitude over a long time range, i.e. the value corresponding to the observed minimum spot coverage. In most cases, the ASAS V-magnitudes are found to be brighter than those reported in the references below.

ϵ *Chamaeleontis*. Colours are taken either from Torres et al. (2006) or Alcalà et al. (1995) both in the Johnson-Cousins photometric system. All but two members (GSC 9235-01702 and CD−74712) are found to be affected by reddening (see online Tables B.3-B.5). The colour excess

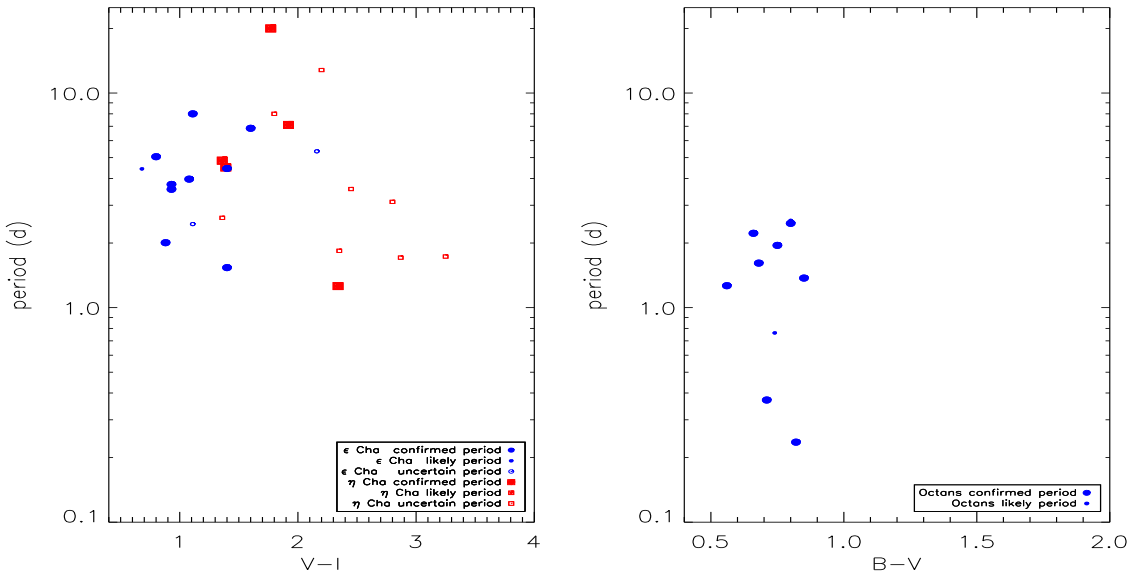

Fig. 4 *left panel:* distribution of rotation period of ϵ/η Cha members versus V−I colour. The V−I colour is used since almost all the η Cha members lack B−V measurements. *Right panel:* same as left panel but for Octans members versus B−V.

of each target is determined by comparing the observed V−I colour with the V−I colour corresponding to the spectral type of a standard dwarf star. The A_V extinction is derived from E(V−I) using the relations of Mathis (1990). We find that the A_V extinction ranges from 0.1 to 1.8 mag. A study by Knude & Hog (1998) based on the Hipparcos and Tycho data found that in the Chamaeleon region the interstellar extinction in the distance range of our targets never exceeds $A_V \sim 0.15$ mag. Therefore, the derived reddening, in agreement with the very young age of the ϵ Cha members, likely arises from circumstellar rather than from interstellar material.

η Chamaeleontis. Colours in the Johnson-Cousins photometric system and spectral types in the present paper are taken from Lawson et al. (2001; 2002). A study by Westin (1985) has found the interstellar reddening for this cluster to be unimportant. This result is also confirmed by Mamajek et al. (2000) who found the V−I colour of members to be consistent with the inferred spectral type.

Octans. The observed colours are taken from Torres et al. (2006) and are found to be consistent with the spectral types; therefore, no reddening correction is applied. We adopt the V−I colour corresponding to the target's spectral type for four stars missing V−I measurements. Only one star (TYC 7066 1037 1) with measured V−I colour shows an excess that we corrected as described above.

Argus. V−I colours are taken from Torres et al. (2006). We adopt the colours corresponding to the spectral type of standard dwarf stars for 14 members that lack V−I measurements. Only one star (TYC 8561 0970 1) with measured V−I colour shows an excess that we corrected as above.

IC2391. Colours in the Johnson-Cousins photometric system are taken either from Patten & Simon (1996) or from Platais et al. (2007). In the latter case only B−V is measured and V−I is inferred from spectral type. The mean reddening towards IC 2391 is estimated to be close to zero (Patten & Simon 1996) and no correction was made for interstellar reddening. Only one star (PMM 1759) needed to be corrected to make V−I consistent with spectral type.

In general, as expected from variability arising from spots and/or faculae, the V-magnitude variability amplitude in our targets never exceeds ∼0.3 mag. The only deviating star is PMM 8145 whose variability amplitude reaches ∼2 mag. In this case, however, there is a close, very bright nearby star (o Vel, V=3.6 mag $\Delta\alpha$=2 arcsec, $\Delta\delta$=70 arcsec) and therefore CCD saturation affecting the PMM 8415 time-series cannot be ruled out.

V magnitudes, B−V, and U−B colours (flagged with A_V when corrected for reddening), absolute magnitudes, distances and $v \sin i$ values from the literature are listed in the online Tables B.3-B.5.

The reddening-corrected CMDs of the studied associations are plotted in Figs. 1-2 together with the Baraffe et al. (1998) evolutionary tracks and the CMDs of three well-studied open clusters of known age for reference: α Persei (∼70 Myr), the Pleiades (∼110 Myr), and NGC 2516 (∼150 Myr).

As in Paper I, we estimate masses and radii comparing positions in the CMD with the Baraffe et al. (1998) evolutionary tracks. The stellar radius (R) allows us to make a comparison between $v \sin i$ and the equatorial velocity $v_{eq}=2\pi$ R /P (where P is the rotation period) to check the consistency between the two and derive the stellar inclination. Derived masses and radii are listed in the online Tables B.3-B.5.

5.2. $v \sin i$ vs. equatorial velocity

All but five of the periodic variables in our sample have known projected equatorial velocities ($v \sin i$). In Fig. 3, we compare $v \sin i$ and v_{eq}, by delineating the loci of $v \sin i = v_{eq}$, corresponding to equator-on orientation, and

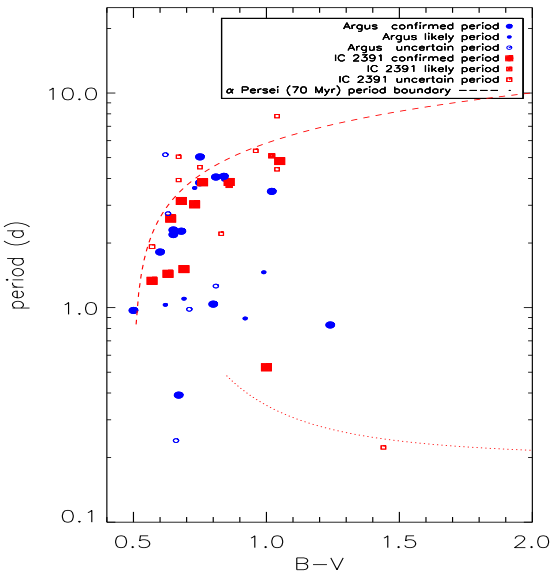

Fig. 5 The same as Fig. 4, but for Argus / IC 2391 association. The dashed and dotted lines represent mathematical functions describing the loci of the upper and lower bounds of the period distribution of α Persei members according to Barnes (2003).

$v \sin i = \pi/4$ v_{eq}, corresponding to a randomly orientated rotation axis distribution. In Fig. 3 all periodic (*confirmed*, *likely*, and *uncertain*) targets are plotted. The major uncertainty in the equatorial velocity is the radius estimate. The reported $v \sin i$ uncertainties are on average 10%. Only four stars (GSC 9419-01065 in ϵ Cha, CD-582194 and CPD-621197 in Argus, and PMM 351 in IC 2391) (flagged with an apex *c* in Tables 2 and 4 and plotted with circled symbols in Fig. 3) have inconsistent $v \sin i / v_{eq}$ (i.e., much larger than unity). These cases are discussed in Appendix A.

In Table 5, for each association we report the average $<\sin i> \pm \sigma$, the correlation coefficient r from the linear Pearson statistics between $v \sin i$ and v_{eq}, where the labels a and b indicate the significance level of the correlation coefficient. The significance level represents the probability of observing a value of the correlation coefficient greater than r for a random sample with the same number of observations and degrees of freedom.

It is interesting to note that all association members have mean inclinations that are inconsistent with the value $(\pi/4)$ expected for a completely randomly orientated rotational axis distribution. Specifically, all association members tend to appear almost equator-on to the observer. This behaviour, which was also exhibited by the six other associations within 100 pc analysed in Paper I, may arise from some bias rather than being real. A bias in the member selection is unlikely, since the association members were identified in larger samples selected on the basis of their X-ray emission, which is not affected by the inclination of the rotation axis. On the contrary, a bias towards equator-on members may be more likely. In fact, we find that members with unknown rotation periods exhibit on average $v \sin i$ systematically smaller than members with *uncertain, likely,* and *confirmed* periods, respectively. In the specific case of Argus / IC 2391, which is the most numerous association in the present paper, we find that members with unknown periods have $<v \sin i>$=15.1 km s^{-1} with respect to $<v \sin i>$=33.8 km s^{-1} exhibited by members with *confirmed* periods. In the case of the AB Dor association studied in Paper I we find $<v \sin i>$=8.2 km s^{-1} for stars with unknown period against $<v \sin i>$=25.9 km s^{-1} for members with *confirmed* periods. From the former case, we can infer that about 20% of stars, whose average $v \sin i$ is about half that of equator-on stars, is still missing in the $v \sin i$ versus v_{eq} plot of Argus / IC 2391. Therefore, a bias towards stars with high values of inclination is present, which are those that show larger-amplitude light modulation and that are most favoured for the rotation period determination. We may also suppose that our derived radii are all systematically underestimated, likely from effects of high magnetic activity and fast rotation, as found by, e.g., Chabrier et al. (2007) and Morales et al. (2009). This makes v_{eq} systematically small with respect to the measured $v \sin i$. Nonetheless, these two quantities are found to be strongly correlated (see Table 5) differently than expected in the case of random distribution of axes. This finding certainly deserves further investigation to take all possible observation biases into account so is beyond the scope of the present paper.

5.3. ϵ / η Chamaeleontis

We determined the rotation periods for 11 stars in ϵ Cha, of which there are ten new and one already known in the literature. The rotation periods of another two stars were retrieved from the literature. For stars in η Cha, we retrieved 12 rotation periods, of which seven were retrieved from the literature. For ϵ and η Cha we therefore have a total of 25 periods available, 14 *confirmed,* 1 *likely,* and 10 *uncertain.* In the left panel of Fig. 4, we plot with filled blue bullets and red squares the members of ϵ and η Cha, respectively, with *confirmed* periods. Small-size filled symbols represent *likely* periods, whereas small-size open symbols are used for *uncertain* periods.

Members of ϵ Cha with *confirmed* periods have all M $\geq$ 0.8M$_\odot$. Their periods have a mean P_{mean} = 4.35d and a median P_{median} = 3.97d. Members of η Cha with confirmed periods have all but one M$\geq$0.8M$_\odot$. Their periods have P_{mean} = 4.67d and P_{median} = 4.84d, although only derived from four stars. If ϵ and η Cha are considered together as a coeval system, we obtain P_{mean} = P_{median} = 4.45d.

5.4. Octans

Of 12 late-type members to the Octans association, we determine the rotation periods of ten stars (eight of which are *confirmed* periods, and two are *likely* periods). The Octans rotation period distribution is plotted in the right panel of Fig. 4. Owing to the very small number of known late-type members, the period distribution upper bound is not sufficiently defined. All *confirmed* periodic members in our study have masses M $\geq$ 0.8M$_\odot$ and the mean and median periods turned out to be P_{mean} = 1.46d and P_{median} = 1.61d.

Octans is the most distant association ($\sim$140 pc) and, owing to the small number of members with accurate trigonometric parallax, its age is the most uncertain in our

sample. As for the other associations, the Octans members were selected by SACY on the basis of their X-ray emission in the ROSAT Bright Survey. However, the detected members of Octans are at the detection limit of that survey. Therefore, it is likely that only the most active and, therefore, fast rotating members have been detected. That means that our sample of periodic stars is biased, the detection of only the fastest rotating stars being favoured. Therefore, the bias towards the faster rotators, together with the uncertainty on age, makes the Octans mean and median rotational periods quite unreliable, which must be taken into account in our analysis of the rotation period evolution reported in Fig. 7.

5.5. Argus / IC 2391

Among the three associations under analysis, Argus has the largest number of late-type members, 27 Argus stars plus 30 additional stars in the IC 2391 cluster. We determine the rotation period of 45 members. However, only for 23 members, which are plotted in Fig. 5, are the rotation periods *confirmed*.

We overplot the empirically determined functions computed according to Barnes (2003) and describing the loci of the upper/lower bounds of the α Persei period distribution for main-sequence stars. The Argus/IC 2391 upper bound is very close to the dashed line, which is computed for a nominal age of 70 Myr, suggesting an age for Argus/IC 2391, slightly older than the quoted age of 40 Myr. Considering *confirmed* periods only, we found $P_{mean} = P_{median} = 2.27$d for Argus, $P_{mean} = 2.36$d, and $P_{median} = 3.03$d for IC 2391. In both cases all stars have mass $M > 0.8 M_{\odot}$. When all members (Argus/IC 2391) are considered, together $P_{mean} = 2.43$ and $P_{median} = 2.30$d. Although quoted with the same age, we see, either in Fig. 5 or from the above mean values, that the distribution of rotation periods of IC 2391 stars appears slightly different from that of Argus stars, with more slow rotators in the cluster. This difference may arise from the different selection criteria adopted to search for members. Argus members are identified on the basis of their X-ray emission and are all present in the ROSAT Bright Source Catalog (Voges et al. 1999). Conversely, the IC 2391 members are selected from a variety of sources, without X-ray preselection. Since fast rotators have brighter coronal luminosities and the mean distance of Argus association members is 106 pc, compared to ∼145 pc for IC 2391, we expect that the census of association members is biased toward the most active and fast-rotating stars (see Desidera et al. 2011).

5.6. Rotation-photospheric activity connection

Following Paper I, we have extracted for each *confirmed* periodic target the V-band maximum peak-to-peak light curve amplitude ever observed in the available time series that are plotted in Fig. 6. For the older associations under analysis, Octans and Argus/IC 2391, the photometric variability mostly arises from the presence of cool spots on the stellar photosphere. In the case of ϵ/η Cha, a contribution from hot spots, arising from accretion processes, cannot be ruled out. The largest amplitudes are observed in the youngest association at an age of about 6 Myr where the presence of circumstellar material (as inferred from the observed colour excess) and related accretion phenomena are still expected. The lowest amplitudes are observed in the Octans association with an assumed age of about 20 Myr. The apparent age dependence of the light curve amplitude at fixed rotation and mass will be discussed in a forthcoming paper (Messina et al., in preparation).

5.7. Rotation period evolution

In Fig. 7, we plot the results of our period search in the nine associations under study, where we show the rotation period variation of low-mass stars versus age in the 0.8-1.2 $M_{\odot}$ range. We plot the rotation periods listed in Tables 2-4 of this paper, and in Tables 3-8 of Paper I, complemented with the updated values listed in Table B.1 of this paper. We overplot the median and mean rotation periods computed for each association (or coeval associations as explained by the labels) considering only the *confirmed* rotation periods to which we assign the same weight. We also add the mean and median rotation periods of ONC (Herbst et al. 2002), NGC 2264 (Rebull et al. 2002; Lamm et al. 2004), α Persei, and the Pleiades, whose rotation periods are taken from the compilation of Messina et al. (2003, and references therein).

In Table 6 we report for each cluster/association the number of confirmed periods used to derive the mean and median values, as well as the KS significance levels that consecutive (at increasing ages) measured period distributions are drawn from the same distribution according to Kolmogorov-Smirnov tests (see, e.g., sect. 14.3 of Press et al. (1992). Period distribution variations that are not statistically significant have KS values close to unity, while statistically significant variations have KS values close to zero.

The newly added mean and median values at 6 Myr (ϵ/η Cha) and 40 Myr (Argus/IC 2391) confirm the trend of period evolution with age found in Paper I. From 1 to 9 Myr, the mean and median periods slowly decrease, but the KS values remain rather high, which indicate that indeed the period distributions do not change significantly. This behaviour is consistent with a locking mechanism operating in this age range. From 9 to 30 Myr both mean and median periods decrease and the KS values indicate a statistical significant variation in this case. The decrease in mean and median periods is monotonic, with only the period distribution of Octans deviating from this trend. However, as discussed in Sect. 5.4, the sample of known Octans late-type components is expected to be rather incomplete and biased towards fast rotators, which could explain the rather low mean and median periods compared with adjacent values. Furthermore, the Octans age uncertainty is considerably larger than for the other associations. For the 0.8 - 1.2 $M_{\odot}$ range, our analysis is therefore consistent with a considerable disc-locking before 9 Myr, followed by a moderate but unambiguous spin-up from 9 to 30 Myr, consistent with stellar contraction towards the ZAMS.

Variations between 30 and 70 Myr are rather doubtful. The KS test indicates that there is no significant variation between 30 and 40 Myr. On the other hand, the KS test indicates a significant variation between 40 and 70 Myr, but while the median indicates a significant spin-up, the mean remains approximately constant. Between 70 and 110 Myr the KS test indicates a significant variation and both mean and median periods increase. This situation may be due to

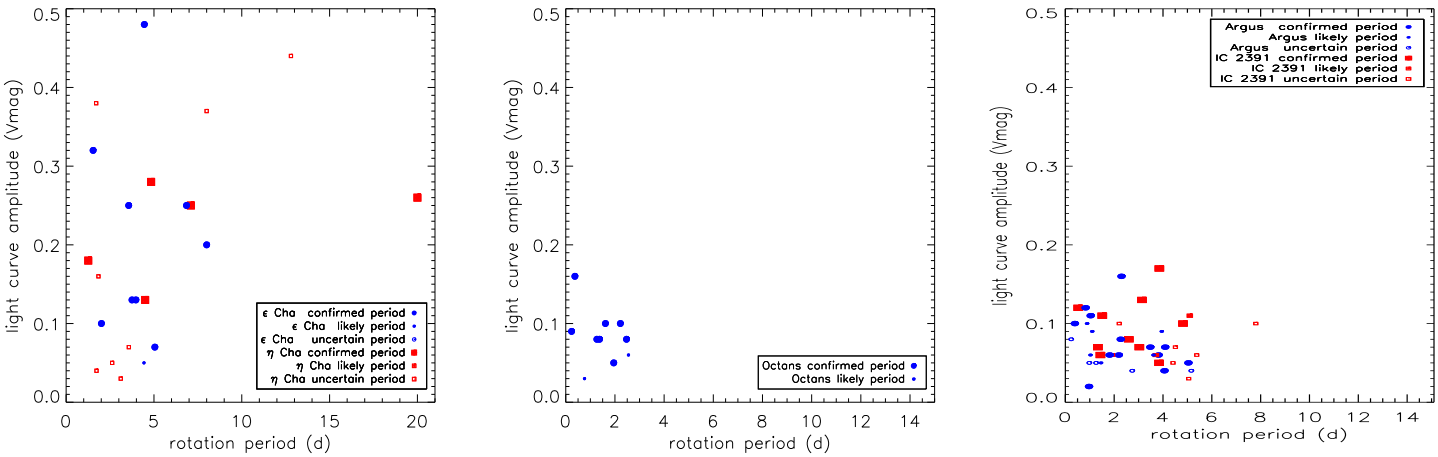

Fig. 6 Distribution of V-band peak-to-peak light curve amplitudes versus rotation period for the members of ϵ/η Cha (left panel), Octans (middle panel), and Argus/IC 2391 (right panel.)

the heterogeneity of the sample: all stars with masses above 1 $M_\odot$ are expected to complete their contraction toward the ZAMS at ages earlier than about 30 Myr, but stars with lower mass will end the contraction towards the ZAMS later on (around 70 Myr for a star of 0.8 $M_\odot$). The unambiguous spin-down from 70 to 110 Myr is consistent with all stars in the 0.8 - 1.2 $M_\odot$ mass range having entered the MS phase and therefore the angular momentum evolution being dominated by wind-braking.

6. Conclusions

We have performed a rotation period search for all late-type members of the nine young (<100 Myr) associations known to date for which either ASAS or SuperWASP data are available. We supplemented such information with rotation periods retrieved from the literature to derive a catalogue that contains (considering also the new periods listed in Table B.1) a total of 241 rotation periods. We have established quality criteria for classifying the derived period based on the frequency of period determination in various light-curve segments, independent measurements retrieved from the literature, and consistency with $v \sin i$. Based on such criteria, three quality levels are proposed: confirmed, likely, and uncertain. Our catalogue contains 171 *confirmed*, 44 *likely*, and 26 *uncertain* periods. The rotation period remains unknown for the remaining 50 late-type members. Thanks to the newly determined period distributions at ∼6, ∼30, and ∼40 Myr, our catalogue allows a better empirical description of angular momentum evolution of stars with masses from 0.8 to 1.2 $M_\odot$ and with ages from 1 to 100 Myr.

The catalogue is used to build rotation period distributions vs. colours for each association in the 0.8-1.0 $M_\odot$ mass range. Excluding Octans, which is likely to be affected by a strong selection bias toward shorter periods, the average and median periods are found to essentially decrease from the ONC age (∼1 Myr) untill the α Persei age (∼70 Myr). The two-sided KS test indicates that indeed the period distributions do not change much from 1 to 9 Myr, while variations are statistically significant from 9 to 30 Myr. This increase in the average rotation rate with age is consistent

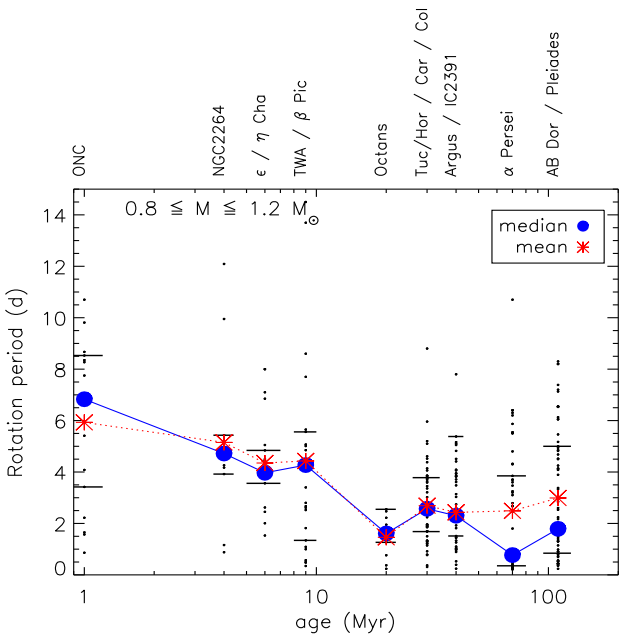

Fig. 7 Rotation period evolution versus time in the 0.8-1.2 solar mass range. Small dots represent individual rotation period measurements. Bullets connected by solid lines are median periods, whereas asterisks connected by dotted lines are mean periods. Short horizontal lines represent the 25th and 75th percentiles of rotation period. This plot updates the right panel of Fig. 12 of Paper I.

with the contraction of the stars toward the ZAMS, which is contrasted by disc-locking at an early stage. The situation from 30 to 70 Myr is rather uncertain, probably because of the heterogeneity of our sample, in which stars of different mass reach the ZAMS at different ages. From α Per (70 Myr) to the AB Dor/Pleiades (110 Myr) both mean and median periods increase with the KS test, indicating a statistically significant variation.

Table 6 Summary of rotation period average values and of Kolmogorov-Smirnov test (KS) results.

		0.6-1.2 $M_\odot$				**0.8-1.2 $M_\odot$**				
Target	Age (Myr)	# Stars	P_{median} (d)	P_{mean} (d)	KS	# Stars	P_{median} (d)	P_{mean} (d)	KS	
ONC	1	33	6.83	6.17	0.57	16	6.83	5.93	0.70	1 vs. 4 Myr
NGC 2264	4	26	5.43	6.19	0.59	10	4.72	5.15	0.63	4 vs. 6 Myr
ϵ / η Cha	6	...	...	...	...	14	3.97	4.35	0.30	6 vs. 9 Myr
TW Hya / β Pic	9	37	4.83	4.75	0.09	21	4.27	4.43	0.02	9 vs. 20 Myr
Octans	20	...	...	...	...	8	1.61	1.46	0.12	20 vs. 30 Myr
Tuc/Hor / Car / Col	30	53	2.72	2.88	0.36	45	2.57	2.69	0.96	30 vs. 40 Myr
Argus / IC 2391	40	...	...	...	...	23	2.30	2.43	0.00	40 vs. 70 Myr
α Persei	70	54	0.77	2.39	0.12	48	0.77	2.49	0.11	70 vs. 110 Myr
AB Dor / Pleiades	110	75	1.49	2.73	...	49	1.79	2.99	...	...

Acknowledgements

The extensive use of the SIMBAD and ADS databases operated by the CDS centre, Strasbourg, France, is gratefully acknowledged. We used data from the WASP public archive in this research. The WASP consortium comprises of the University of Cambridge, Keele University, University of Leicester, The Open University, The Queen's University Belfast, St. Andrews University, and the Isaac Newton Group. Funding for WASP comes from the consortium universities and from the UK's Science and Technology Facilities Council. The Authors would like to thank Dr. G. Pojmański for the extensive use we made of the ASAS database. We are grateful to the Referee Dr. James for his valuable comments that allowed us to significantly improve our analysis and its presentation.

References

Alcalà, J. M., Krautter, J., Schmitt, J. H. M. M., et al. 1995, A&AS, 114, 109
Baraffe, I., Chabrier, G., Allard, F., & Hauschildt, P. 1998, A&A, 337,403
Bernhard, K., Bernhard, C., & Bernhard, M. 2009, OEJV, 98, 1
Barnes, S., 2003, ApJ, 586, 464
Barnes, S., 2007, ApJ, 669, 1167
Barnes, S., 2010, ApJ, 722, 222
Bouvier, J. 2007 in Star-disk Interaction in Young Stars, Proceedings IAU Symp. 243 eds. J. Bouvier & I. Appenzeller, p. 231
Bouvier, J. 2008, Proceedings of the Annual meeting of the French Society of Astronomy and Astrophysics Eds.: C. Charbonnel, F. Combes and R. Samadi
Butters, O.W., West, R.G., Anderson, D.R., et al. A&A, 520, L10
Carpenter, J.M., Bouwman, J., & Mamajek, E.E, 2009, ApJS, 181, 197
Chaboyer, B., Demarque, P., & Pinsonneault, M. H. 1995a, ApJ, 441, 865
Chaboyer, B., Demarque, P., & Pinsonneault, M. H. 1995a, ApJ, 441, 876
Chabrier, G., Gallardo, J., & Baraffe, I. 2007, A&A, 472, 17
Chauvin, G., Lagrange, A. -M., Bonavita, M., et al. 2010, A&A, 509, A52
Collier Cameron, A., & Campbell, C. G. 1993, A&A, 274, 309
Collier Cameron, A., Campbell, C. G., & Quaintrell, H. 1995, A&A, 298, 133
Collier Cameron, A., Davidson, V. A., Hebb, L., et al. 2009, MNRAS, 400, 451
Desidera, S., Covino, E., Messina, S., et al. 2011, A&A, 529, A54
da Silva, L., Torres, C.A.O., de la Reza, R. et al. 2009, A&A 508, 833
Doppmann, G., White, R., Charbonneau, D., & Torres, G. 2007, Gemini Science 2007, ed. A. Bruch & I. Fernandez, Poster in Proc. of the 2nd Conf. on Gemini Science Results
Feigelson, E. D., Lawson, W. A., & Garmire, G. P. 2003, ApJ, 599, 1207
Feigelson, E. D., Hornschemeier, A. E., Micela, G., et al. 2004, ApJ, 611, 1107
Frink, S., Roeser, S., Alcalá, J.M., et al. 1998, A&A, 338, 442
Giampapa, M. S., Hall, J. C., Radick, R. R., & Baliunas, S. L. 2006, ApJ, 651, 444
Guenther, E. W., Esposito, M., Mundt, R. et al. 2007, A&A, 467, 1147
James, D. J., Barnes, S. A., Meibom, S., et al. 2010, A&A 515A, 100
Jeffries, R. D., & Oliveira, J. M. 2005, MNRAS, 358, 13
Haisch, K. E., Jr., Lada, E. A., & Lada, C. J. 2001, ApJ. 553, 153
Hartman, J. D., Bakos, G. A., Kovàcs, G., & Noyes, R. W., 2010, MNRAS, 408, 475
Hartman, J. D., Gaudi, B. S., Pinsonneault, M. H., et al. 2009, ApJ, 691, 342
Herbst, W., & Wittenmyer, R. 1996, BAAS, 28, 1338
Herbst, W., Bailer-Jones, C. A. L., & Mundt, R. 2001, ApJ 554, 197
Herbst, W., Bailer-Jones, C. A. L., Mundt, R., Meisenheimer, K., & Wackermann, R. 2002, A&A, 396, 513
Herbst, W., & Mundt, R. 2005, ApJ, 633, 967
Herbst, W., Eislöffel, J., Mundt, R., & Scholz, A. 2007, Protostars and Planets, V. B. Reipurth, D. Jewitt, and K. Keil (eds.), University of Arizona Press, Tucson, 951, p.297-311
Hodgkin, S.T., Irwin, J.M., Aigrain, S., et al. 2006, AN, 327, 9
Irwin, J.,& Bouvier, J. 2009, ,The Ages of Stars, Proceedings of the International Astronomical Union, IAU Symposium, Volume 258, p. 363-374
Kawaler, S. D. 1988, ApJ, 333, 236
Kiss, L.L., Moor, A., Szala, T., et al. 2011, MNRAS, 411, 117
Knude, J., & Hog, E. 1998, A&A, 341, 451
Kohler, R. 2001, AJ, 122, 3325
Koenigl, A. 1991, ApJ, 370, 39
Krishnamurthi, A., Pinsonneault, M. H., Barnes, S., & Sofia, S. 1997, ApJ, 480, 303
Lanza, A.F. 2010, A&A, 512, A77
Lamm, M. H., Bailer-Jones, C. A. L., Mundt, R., Herbst, W., & Scholz, A. 2004, A&A, 417, 557
Lawson, W.A., Crause, L.A., Mamajek, E.E., & Feigelson, D.E. 2001, MNRAS, 321, 57
Lawson, W.A., Crause, L.A., Mamajek, E.E., & Feigelson, D.E. 2002, MNRAS, 329, 29
Makarov, V.V., & Urban, S. 2000, MNRAS, 317, 289
Makidon, R. B., Rebull, L.M., Strom, S.E., Adams, M.T., & Patten, B. M. 2004, AJ, 127, 2228
Mamajek, E.E., Lawson, W.A., & Feigelson, E.D. 1999, ApJ, 516, L77
Mamajek, E. E., Lawson, W.A., & Feigelson, E. D. 2000, ApJ, 544, 356
Mamajek, E. E., & Hillenbrand, L. A. 2008, ApJ, 687, 1264
Marsden, S.C., Carter, B.D., & Donati, J.-F. 2009, MNRAS 399, 888
Mathis, J.S. 1990, ARA&A, 28, 37
Matt, S., & Pudritz, R. E. 1995, ApJ, 632, 135
Matt, S.P., Pinzón, G., de la Reza, R., Greene, T. P. 2010, ApJ, 714, 989
Meibom, S., Mathieu, R. D., & Stassun, K.G. 2009, ApJ, 695, 679
Messina, S., Pizzolato, N., Guinan, E. F., & Rodonò, M. 2003, A&A,410, 671
Messina, S. Rodonò, M., & Cutispoto, G., 2004, AN, 325, 660
Messina, S., 2007, Memorie Società Astron, It., 78, 628
Messina, S., Distefano, E., Parihar, P., et al. 2008, A&A, 483, 253
Messina, S., Parihar, P., Koo, J.-R., et al. 2010a, A&A, 513, A29
Messina, S., Desidera, S., Turatto, M., Lanzafame, A.C., Guinan, E.F. 2010b, A&A, 520, A15 (Paper I)
Mestel, L., & Spruit, H. C. 1987, MNRAS, 226, 57

Morales, J. C., Torres, G., Marschall, L. A., & Brehm, W. 2009, ApJ, 707, 671
Norton, A. J., Wheatley, P. J., West, R. G., et al. 2007, A&A, 467, 785
Pace, G., & Pasquini, L. 2004, A&A, 426, 1021
Patten, B.M. & Simon T. 1996, ApJS 106, 489
Platais, I., Melo, C., Mermilliod J.C., et al. 2007, A&A, 461, 509
Pojmanski G., 1997, Acta Astronomica, 47, 467
Pojmanski G., 2002, Acta Astronomica, 52, 397
Pollacco, D., Skillen, I,, Collier Cameron, A., et al. 2006, PASP 118, 848
Pont, F. 2009, MNRAS, 396, 1789
Pontoppidan, K. M., Salyk, C., Blake, G,A., et al. ApJ, 2010, 720, 887
Press, W. H., Teukolsky, S. A., Vetterling, W. T., & Flannery, B. P. 1992, Numerical recipes in FORTRAN. The art of scientific computing, Cambridge: University Press, 2nd ed.
Radick, R. R., Thompson, D. T., Lockwood, G. W., Duncan, D. K., & Baggett, W. E. 1987, ApJ, 321, 459
Randich, S., Bragaglia, A., Pastori, L., et al. 2005, The Messenger, 121, 18
Rebull, L.M. 2001, AJ, 121, 1676
Rebull, L. M., Makidon, R. B., Strom, S. E., et al. 2002, AJ, 123, 1528
Scargle, J.D. 1982, ApJ, 263, 835
Sestito, P., & Randich, S. 2005, A&A, 442, 615
Setiawan, J., Weise, P., Henning, Th., et al. 2008, in Precision Spectroscopy in Astrophysics, Edited by N.C. Santos, L. Pasquini, A.C.M. Correia, and M. Romaniello, p. 201 (arXiv 0704.2145)
Shu, F., Najita, J., Ostriker, E., et al. 1994, ApJ, 429, 781
Skumanich, A. 1972, ApJ, 171, 565
Stassun, K.G., Mathieu, R.D., Mazeh, T., & Vrba, F. 1999, AJ, 117, 2941
Tamuz, O., Mazeh, T., & Zucker, S. 2005, MNRAS, 356, 1466
Torres, C.A.O., Quast, G.R., de la Reza, R., et al. 2003, Astroph. Sp. Sci. Libr. 299, Open Issues in Local Star Formation, ed. J. Lepine & J. Gregorio-Hetem (Kluwer Academic Publishers), 83
Torres, C.A.O., Quast, G.R., da Silva, L. et al. 2006, A&A, 460, 695
Torres, C.A.O., Quast, G.R., Melo, C.H.F., & Sterzik, M.F. 2008, Handbook of Star Forming Regions, Volume II: The Southern Sky ASP Monograph Publications, Vol. 5. Edited by Bo Reipurth, p.757 (arXiv:0808.3362)
Voges, W., Aschenbach, B., Boller, Th. et al. 1999, A&A, 349, 389
von Braun, K., Lee, B.L., Seager, S., et al. 2005, PASP, 117, 141
Weber, E. J., & Davis, L. Jr. 1967, ApJ, 148, 217
Westin, T.N.G. 1985, A&AS, 60, 99
Zuckerman, B. & Song, I. 2004, Ann. Rev. Astron. Astr., 42, 685

Appendix A: Individual stars

A.1. $\epsilon + \eta$ Cha

GSC 9419-01065: the rotation period derived from our analysis is P=8.0d. Although the flux rotational modulation is clearly found in more than five segments; however, the computed $v_{eq}=2\pi R/P$ is inconsistent with the measured $v \sin i$=18.0 km s^{-1} (Torres et al. 2006), so this period is considered *uncertain*. However, we note that the only available $v \sin i$ measurement has quite a large ±30% uncertainty. More accurate determinations would be desiderable to confirm the correctness of the current $v \sin i$ value.

HD 104237E: the ASAS photometry did not allowed us to infer any periodicity. We adopted the period of P=2.45d detected by Feigelson et al. (2003), which combined with the estimated radius gives an equatorial velocity consistent with the measured $v \sin i$. This star belongs to a quintuple system, where the brightest component is the Herbig Ae star HD 104237. Feigelson et al. (2003) found a reddening A_V=1.8±0.3 that likely arises from material within the parent stellar system, the reddening of other members associated to ϵ Cha being small or even absent.

GSC 9416-1029: Doppmann et al. (2007) report a period of P=5.35d that likely represents the system's orbital period. The available ASAS photometry of this star, which is quite inaccurate owing to the target's faintness, shows evidence of a period P=5.50d in two of nine time segments. In the case this is the correct rotational period, which would imply a rotational/orbital synchronisation, which is quite a surprising circumstance at an age of about 6 Myr.

GSC 9235-01702: it has very recently been discovered to be a member of ϵ Cha by Kiss et al. (2011) as part of the RAVE project. From the ASAS photometry, we found the same rotation period as found by Bernhard et al. (2009), based on the same ASAS data.

RECX 1 (EG Cha): we detect a rotation period P=4.5d in 12 of 15 time segments, which is twice the period reported by Lawson et al. (2001). An inspection of Fig. 2 of Lawson et al. (2001) shows that their phased light curves in both 1999 and 2000 seasons exhibit significant magnitude phase dispersion.

RECX 11 (EP Cha): we found a period P=4.84d in 7 of 12 time segments with confidence level over 99% and no evidence of any power peak at the period P=3.95d discovered by Lawson et al. (2001) in 1999 (P=3.69d in 2000). Again, an inspection of their phased light curves shows significant dispersion

RECX 12 (EQ Cha): the star shows two significant periods in Lawson et al. (2001), P=1.25d and P=8.55d. The star is a close binary, so they might represent the rotational periods of the two components. Our analysis allowed us to detect only the shorter period that is adopted in the present analysis.

RECX 15 (ET Cha): is a classical T Tauri star, with evidence of on going accretion (Lawson et al. 2002). The large amplitude variations (up to 0.44 mag) are likely driven by accretion hot spots.

A.2. Octans

CD-58 860: we find two periods, P=1.612d and P=2.610d, in eight out of ten time segments with comparable levels of confidence. However, the longer period, once combined with stellar radius, determines a ratio $v \sin i/v_{eq}$ slightly greater than unity. Therefore, in the present analysis we adopt P=1.612d.

CD-43 1451: this star is also present in the SuperWASP archive. However, neither from the ASAS nor from the SuperWASP database we could determine the rotation period, but only the presence of light variability.

HD 274576: the period P=2.22d is found in nine out of ten time segments of ASAS photometry and in two out of two SuperWASP observation seasons, and it is fully consistent with the measured $v \sin i$. We note that in both the ASAS and SuperWASP timeseries another period P=1.824d is also found with a very high confidence level, although it is smaller than the earlier, in almost all time segments, which is also consistent with $v \sin i$.

TYC 7066 1037 1: the period P=2.47d is found in 6 out of 14 time segments of ASAS photometry and in three out of five segments of SuperWASP photometry.

A.3. Argus and IC 2391

HD 5578 (BW Phe): is a close visual binary. We found two rotation periods of comparable power, P=1.461d

and P=3.15d, in most time segments. The shorter period is assumed to be the star's rotation period, since it is the only one consistent with a $v \sin i/\mathrm{v_{eq}} \leq 1$.

CD-56 1438: we detect a period P=0.24d in only one segment that may conciliate with the very high $v \sin i$.

CD-28 3434: the P=3.82d period is very well established and also detected in three out of three time segments of SuperWASP data, as well in the complete timeseries. Although no $v \sin i$ is available to check consistency with $\mathrm{v_{eq}}$, it is considered a *confirmed* period.

HD 61005: has been suggested to be a likely member of the Argus association (Desidera et al. 2011). Although its P=5.04d period is found in only three time segments of the ASAS timeseries, it was confirmed by the period search carried out in the Tycho and Hipparcos photometry (Desidera et al. 2011), so it is considered *confirmed* in the present analysis.

CD-39 5883: the period is detected in two out of nine segments of ASAS photometry and in five out of five segments of WASP data as well in the complete timeseries and is consistent with $v \sin i/\mathrm{v_{eq}} \leq 1$.

CD-58 2194: the most significant period is P=5.16 detected in four time segments as well in the complete timeseries. However, it is inconsistent with the high $v \sin i$. It may be the beat of the P=0.55d period detected in only one season. This period is therefore considered *uncertain.*

CD-57 2315: it is variable, but no periodicity was found.

CPD-62 1197: the most significant period is P=1.26d which is found in seven out of nine segments. However, it leads to a $v \sin i/\mathrm{v_{eq}} \sim 2$ and therefore it will not be considered in the following analysis. Another significant period is P=0.82d, which is, however only detected in three out of nine segments, so it is classified as *uncertain.*

TYC 7695 0335 1: the same P=0.39d is found in three out of nine ASAS segments and in four out of four segments of SuperWASP data.

HD85151A: is a close visual binary. The P=0.97d is only found in the ASAS complete timeseries, but in five out of five time segments of SuperWASP data.

CD-65 817: is a close visual binary.

HD 310316: is a close visual binary.

CD-74 673: is a spectroscopic binary with an orbital period P=614d (Guenther et al. 2007).

CD-52 9381: the most significant period is P=5.19d detected in six out of nine time segments, as well in the complete series. However, a P=0.89d is also detected and reported in the ACVS. The shorter one is consistent with $v \sin i/\mathrm{v_{eq}} \leq 1$, and it is considered as a *confirmed* period.

PPM 351: the most significant period is P=1.931d that is found in six out of nine segments; however, it gives $v \sin i/\mathrm{v_{eq}} > 1$. Another detected period is P=0.69d, which is, however, found in only three out of nine segments, so it is considered *uncertain.*

PMM 1083 (V365 Vel): our period determination is in good agreement with the earlier determination by Patten & Simon (1996). Two different $v \sin i$ values are reported in the literature, $v \sin i$=43 $\mathrm{kms^{-1}}$ from Marsden et al. (2009) and $v \sin i$=67 $\mathrm{kms^{-1}}$ from Platais et al. (2007). However, only the first is consistent with $v \sin i/\mathrm{v_{eq}} \leq 1$.

PMM 1820 (V366 Vel): our period determination is in good agreement with the earlier determination by Patten & Simon (1996).

PMM 4413: is an SB2 with an orbital period P=90.6d (Platais et al. 2007) whose components have measured $v \sin i$ of 8.6 and 8.4 $\mathrm{kms^{-1}}$, which give consistent $v \sin i/\mathrm{v_{eq}}$ ratios.

PMM 4467 (V364 Vel); PMM 4902; PMM 5884 (V377 Vel): our period determinations are in good agreement with the earlier determinations by Patten & Simon (1996).

PPM 8145: unlike stars whose variability arises from dark spots, this star spends most of its time in its fainter state. The variability likely arises from magnitude outbursts. It shows the largest variability amplitude ($\sim$ 2 mag) in our sample. The reference magnitude, differently than other stars, is probably the faintest one.

PMM 4902 (V379 Vel): although detected in only three time segments, it is considered *confirmed* because its period is confirmed by the literature value (Patten & Simon 1996).

PPM 2182: we found two significant periods, P=3.28d and P=1.437d. However, both are not consistent with $v \sin i/\mathrm{v_{eq}} \leq 1$, being $v \sin i$=78 $\mathrm{kms^{-1}}$ (da Silva et al. 2009) and therefore are considered *uncertain.*

Appendix B: New/revised periodicities in young associations studied in Paper I

The availability of SuperWASP light curves allowed us to revisit some of the targets studied in Paper I. We found SuperWASP timeseries for 71 targets listed in Paper I. For the seven candidate members of β Pic and Tuc/Hor newly proposed by Kiss et al. (2011), we retrieved SuperWASP timeseries for two of them and ASAS time series for the remaining five. Unfortunately, of 78 targets the data on nine stars turned out to be too sparse to be suitable for a meaningful period search. The analysis of the 69 timeseries allowed us to discover (*i*) 15 new periods (5 of which *likely*), (*ii*) to confirm 35 periods, and (*iii*) to revise 13 periods. Finally, for six stars we could not detect any period. Three of them were also found non periodic in Paper I, two were found periodic in only 1 or 2 ASAS time segments, and one had only one literature determination. Our results are summarised in Table B.1.

Concerning the revised periods, the previous determinations reported in Paper I were either based on literature values (1 target), had inconsistent $v \sin i/\mathrm{v_{eq}}$ ratio (4 targets), or were beat periods detected in less than five time segments (5 targets), or detected in five or more segments (3 targets). Based on this result for the period revision of a few targets in Paper I, in the present work we decided to consider a rotation period to be well established (*confirmed*) if detected in five or more time segments or in fewer, but with an independent determination from the literature.

In the following we update the results presented in Paper I including new results based on Super WASP and on a more conservative period selection.

TW Hydrae

We found SuperWASP data for eight targets in TW Hya and confirmed the rotation periods of four targets, and determined three new periods. However, only one out of the three newly periodic targets (TWA 20) is a confirmed TWA member, the other two having been rejected or needing to be confirmed. The rotation period of TWA 23,

although detected in three out of five time segments, has a critical value close to the data 1-day observation sampling. Therefore, even if reported in this work, it needs additional observations to be confirmed, therefore, we classify it as *uncertain.*The data of TWA 3 were quite sparse to be suitable for a period search.

To summarise, we have so far derived *confirmed* periods for 15 out of 17 certain late-type members of TW Hya. Rotation periods of TWA 3A and TWA 3B are still unknown.

β Pictoris

Data for 13 β Pic targets are available in the SuperWASP database, five of which have been recently identified as β Pic members by Kiss et al. (2011). For seven targets we confirm the period determined in Paper I. For the other six we determined previously unknown period, five of them classified as *confirmed,* the other one (J01071194-1935359) as *likely.*

To summarise, we derived *confirmed* periods for 29 of the 37 late-type members of β Pic. For a further three stars we determined *likely* periods, whereas for only one star we have an *uncertain* period. The rotation periods of four stars still remain unknown.

Tucana/Horologium

Data for 19 Tucana/Horologium targets are available in the SuperWASP database, two of which have been recently identified as Tucana/Horologium members by Kiss et al. (2011). For nine targets we confirm the rotation periods determined in Paper I. For one target (J01521830-5950168) we determined the previously unknown period that we classify as *uncertain.*We revised the period of HIP 21632, which was taken from the literature in Paper I and based on Hipparcos photometry, and the period of TYC 8852 0264 1 whose earlier determination led to inconsistent $v \sin i/\mathrm{v_{eq}}$ ratio. This star was excluded in Paper I from rotation period evolution analysis also because it is a rejected member. SuperWASP data of six targets were quite sparse and unsuited for period search. Data of HD 25402 were suited but did not allow any period detection.

To summarise, we derived *confirmed* periods for 22 of 29 late-type members of Tucana/Horologium. Two stars have rotation periods still to be confirmed. Rotation periods of five stars HIP 490 HIP 6856, TYC 8489 1155 1, AF Hor, and HIP 16853 are still unknown.

Columba

Data for 12 Columba targets are available in the SuperWASP database. For four targets we confirm the rotation period determined in Paper I. For two targets we determined the previously unknown period that we classify as *confirmed.* We revised five rotation periods. The revised period of TYC 7100 2112 1 now gives consistent $v \sin i/\mathrm{v_{eq}}$ ratio. The other four revised periods were in Paper I either beat periods or detected in four or fewer time segments, whereas they are now well established. Data of HIP 25709 were too sparse to allow a period determination.

To summarise, we derived *confirmed* periods for 20 of 23 late-type members of Columba. TYC 6457 2731 1 and TYC 5346 132 1 still have unknown periods. The period of HIP 25709 is classified as *likely.*

Carina

We did not find any SuperWASP data for the Carina late-type members. We derived *confirmed* periods for 14 of 21 late-type members. Four stars have the period classified as *likely.* The periods of TYC 8584 2682 1, HD107722 is still unknown. TYC 8586 2431 1 has period leading inconsistent $v \sin i/\mathrm{v_{eq}}$ ratio.

AB Doradus

Data for 26 AB Doradus targets are available in the SuperWASP database, and for three targets we determined the previously unknown period (one classified as *confirmed*, and two as *likely*). For 11 targets we confirm the rotation period determined in Paper I. We revised six periods, and did not detect any periodicity of five stars although the timeseries are suitable for the period search. The observations of one target are too sparse for period search. The rotation period of HIP 116910 reported in Paper I revealed itself to be the beat period of the *confirmed*P=1.787d discovered in SuperWASP data. The periods of TYC 7059 1111 1 and TYC 7598 1488 1 reported in Paper I led to inconsistent $v \sin i/\mathrm{v_{eq}}$ ratio, whereas the updated period solved the inconsistency. The period of TYC 7064 0839 1, TYC 7605 1429 1, and TYC 7627 2190 1 reported in Paper I were detected in less than five time segments, whereas the new periods are classified as *confirmed*.

To summarise, we derived *confirmed* periods of 29 of 64 late-type members of AB Doradus. Twenty members have periods classified as *likely.* The rotation period of 15 members is still unknown.

In Figs. B.1-B.3 we plot the updated rotation period distributions in the young associations studied in Paper I, where the newly discovered and the revised rotation periods are plotted with squared and squared crossed symbols, respectively, whereas circled symbols represent the rotation periods of the new candidate members proposed by Kiss et al. (2011).

Similarly, in Fig. 6 we plot the updated distributions of light curve amplitudes versus rotation period in the young associations studied in Paper I.

We notice that both rotation periods and light curve amplitudes of the newly proposed members by Kiss et al. (2011) agreet with the values of the other confirmed association members. This evidence gives further support to their assigned membership.

Table B.1 Summary of period search of 71 targets in Paper I and of seven recently added members with photometry timeseries in the SuperWASP archive.

Name	SuperWASP/ASAS ID	P (d)	ΔP (d)	Timeseries Segments	Note on Period
TW Hydrae					
TWA 3AB	1SWASP J111027.90-373152.0	...	...	...	sparse observations
TWA 6	1SWASP J101828.70-315002.8	0.542	0.002	4/5	confirmed
TWA 8	1SWASP J113241.23-265200.7	4.64	0.04	4/4	confirmed
TWA 9	1SWASP J114824.21-372849.2	5.01	0.1	6/6	confirmed
TWA 13	1SWASP J112117.43-344647.1	5.50	0.06	5/5	confirmed
TWA 16	1SWASP J123456.31-453807.4	1.078	0.007	4/6	new
TWA 20	1SWASP J123138.06-455859.3	0.647	0.002	5/6	new
TWA 23	1SWASP J120733.91-324652.8	1.033	0.003	3/5	new (to be confirmed)
β Pictoris					
TYC 1186 706 1	1SWASP J002334.66+201428.6	7.9	0.5	5/5	confirmed
BD-21 1074	1SWASP J050649.47-213503.7	13.4	0.4	4/4	confirmed
TYC 6878 0195 1	1SWASP J191144.66-260408.5	5.70	0.06	4/5	confirmed
HIP 102141	1SWASP J204151.15-322606.7	1.197	0.005	3/6	new
HIP 102409	1SWASP J204509.52-312027.2	4.84	0.04	2/3	confirmed
TYC 2211 1309 1	1SWASP J220041.59+271513.5	0.5229	0.0006	6/6	confirmed
HIP 112312	1SWASP J224457.83-331500.6	2.35	0.01	6/6	confirmed
HIP 11437	1SWASP J022729.25+305824.6	12.5	0.3	6/6	confirmed
J01071194-1935359	ASAS 010713-1935.4	7.26	0.07	2/11	new (to be confirmed)
J16430128-1754274	ASAS 164301-1754.4	5.14	0.04	5/14	new
HD160305	ASAS 174149-5043.5	1.341	0.008	13/21	new
TYC 7443 1102 1	1SWASP J195604.37-320737.7	11.8	0.2	5/5	new (also found in ASAS)
J20013718-33131391	1SWASP J200137.17-331313.7	12.7	0.2	5/5	new
Tucana/Horologium					
HIP 1113	1SWASP J001353.01-744117.8	...	...	...	sparse observations
HIP 116748	1SWASP J233939.48-691144.8	...	...	...	sparse observations
HIP 1910	1SWASP J002408.97-621104.4	1.755	0.005	3/3	confirmed
HIP 1993	1SWASP J002514.55-613047.8	4.33	0.03	3/3	confirmed
HIP 21632	1SWASP J043843.94-270201.8	2.32	0.01	2/2	P revised ($P \neq P_{lit}$)
HIP 2729	1SWASP J003451.19-615458.1	...	...	...	sparse observations
HIP 490	1SWASP J000552.54-414511.0	...	...	...	sparse observations
HIP 9141	1SWASP J015748.97-215405.3	3.02	0.03	3/4	confirmed
TYC 5907 1244 1	1SWASP J045230.53-200013.2	...	...	...	sparse observations
TYC 7026 0325 1	1SWASP J031908.66-350700.3	8.5	0.1	4/4	confirmed
TYC 7048 1453 1	1SWASP J051829.04-300132.0	1.7	0.1	2/4	confirmed
TYC 7065 0879 1	1SWASP J054234.25-341542.2	3.81	0.08	4/4	confirmed
TYC 7574 0803 1	1SWASP J033155.65-435913.5	2.92	0.01	3/3	confirmed
TYC 7600 0516 1	1SWASP J053705.31-393226.3	2.46	0.01	4/4	confirmed
TYC 8060 1673 1	1SWASP J033049.09-455557.3	3.77	0.02	3/3	confirmed
TYC 8852 0264 1	1SWASP J011315.34-641135.1	1.265	0.003	3/3	P revised
TYC 9344 0293 1	1SWASP J232610.70-732349.9	...	...	...	sparse observations
J01521830-5950168	ASAS 015220-5950.4	6.35	0.06	2/15	new (to be confirmed)
HD 25402	ASAS 040032-4144.9	...	...	...	undetected
Columba					
HIP 16413	1SWASP J033120.80-303058.7	1.856	0.006	3/4	revised
HIP 19775	1SWASP J041422.57-381901.5	1.684	0.006	4/4	revised
HIP 25709	1SWASP J052924.10-343055.5	...	...	...	sparse observations
TYC 6502 1188 1	1SWASP J055021.43-291520.7	3.45	0.02	4/4	revised
TYC 7044 0535 1	1SWASP J043450.78-354721.2	2.29	0.01	4/4	new
TYC 7100 2112 1	1SWASP J065246.73-363617.0	0.307	0.001	3/3	revised
TYC 7558 0655 1	1SWASP J023032.40-434223.3	8.8	0.1	5/5	confirmed
TYC 7584 1630 1	1SWASP J042148.68-431732.5	1.963	0.007	3/4	revised
TYC 7597 0833 1	1SWASP J054516.24-383649.1	1.325	0.003	4/4	new
TYC 7617 0549 1	1SWASP J062606.91-410253.8	4.14	0.03	4/4	confirmed
TYC 8077 0657 1	1SWASP J045153.54-464713.3	2.83	0.01	3/3	confirmed
TYC 8086 0954 1	1SWASP J052855.09-453458.3	4.67	0.04	4/4	confirmed
AB Doradus					
HIP 106231	1SWASP J213101.71+232007.3	0.4232	0.0002	5/5	confirmed
HIP 107684	1SWASP J214848.51-392909.5	4.150	0.006	5/5	confirmed
HIP 113579	1SWASP J230019.28-260913.5	...	...	0/2	undetected
HIP 113597	1SWASP J230027.90-261843.2	8.0	0.1	2/3	new (to be confirmed)
HIP 114530	1SWASP J231152.05-450810.6	5.13	0.05	3/4	confirmed
HIP 116910	1SWASP J234154.29-355839.8	1.787	0.005	4/4	revised
HIP 118008	1SWASP J235610.67-390308.4	...	...	0/4	undetected
HIP 110526A	1SWASP J222329.08+322733.4	0.854	0.003	4/6	new
HIP 12635	1SWASP J024220.95+383721.2	5.3	0.1	2/4	new (to be confirmed)
HIP 14809	1SWASP J031113.84+222457.0	...	...	0/1	sparse data
HIP 16563	1SWASP J033313.48+461526.5	...	...	0/2	undetected
HIP 25283	1SWASP J052430.16-385810.7	9.3	0.1	2/3	confirmed
HIP 26401	1SWASP J053712.91-424255.6	...	...	0/4	undetected
HIP 27727	1SWASP J055215.98-283924.9	2.85	0.01	4/4	confirmed
PW And	1SWASP J001820.88+305722.1	1.76	0.01	3/3	confirmed
TYC 1355 214 1	1SWASP J072343.59+202458.6	2.79	0.03	3/3	confirmed
TYC 6494 1228 1	1SWASP J054413.36-260614.8	...	...	0/4	undetected
TYC 7059 1111 1	1SWASP J052856.52-332815.5	0.694	0.003	3/4	revised
TYC 7064 0839 1	1SWASP J053504.11-341751.9	1.145	0.003	4/4	revised
TYC 7079 0068 1	1SWASP J060833.86-340254.9	3.38	0.02	4/4	confirmed
TYC 7084 0794 1	1SWASP J060919.21-354931.1	1.716	0.005	3/4	confirmed
TYC 7587 0925 1	1SWASP J050230.42-395912.9	6.55	0.08	4/4	confirmed
TYC 7598 1488 1	1SWASP J055750.78-380403.1	0.790	0.004	4/4	revised
TYC 7605 1429 1	1SWASP J054114.34-411758.6	0.3514	0.0001	2/2	revised
TYC 7627 2190 1	1SWASP J064118.50-382036.1	0.726	0.001	4/4	revised
TYC 8042 1050 1	1SWASP J021055.38-460358.6	1.113	0.001	4/4	confirmed

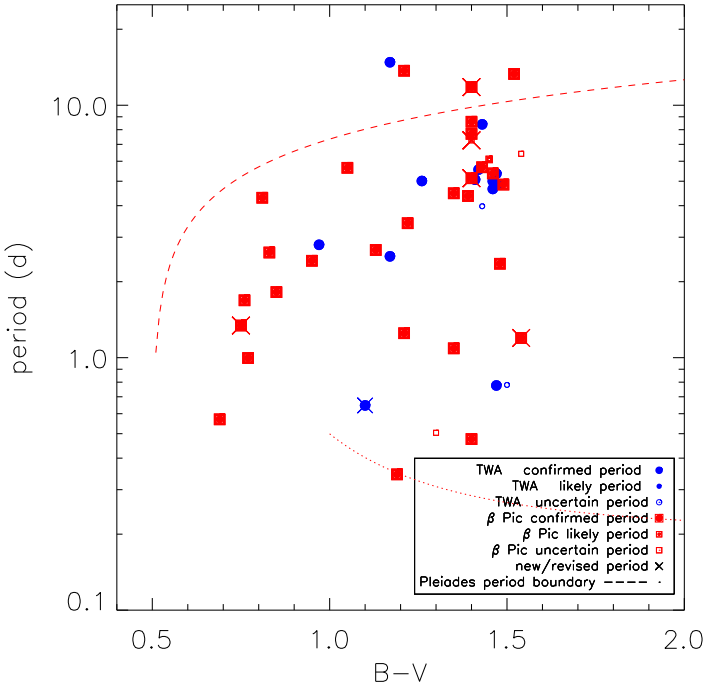

Fig. B.1 Updated distributions of rotation periods in TWA + β Pic associations The dashed and dotted lines represent mathematical functions describing the loci of the upper and lower bounds of the period distribution of the Pleiades members according to Barnes (2003).

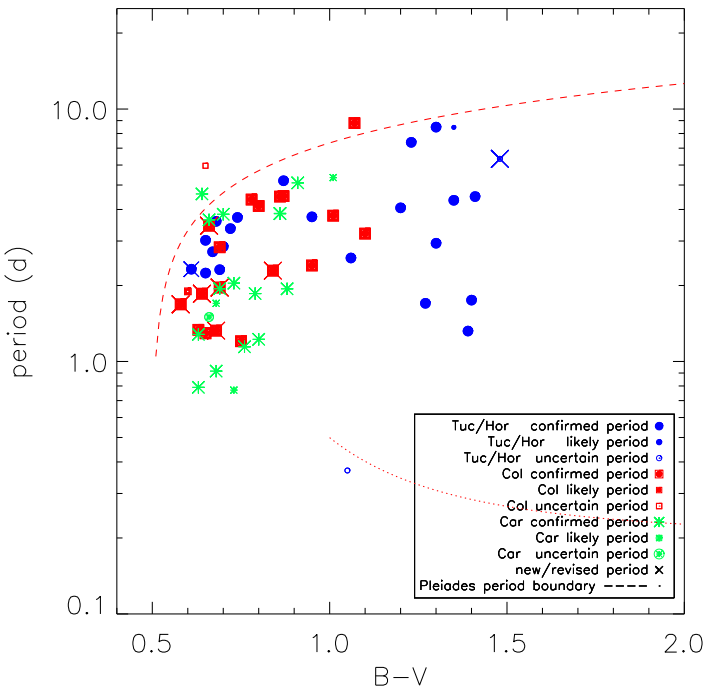

Fig. B.2 As in Fig. B.1 for Tuc/Hor + Car + Col associations.

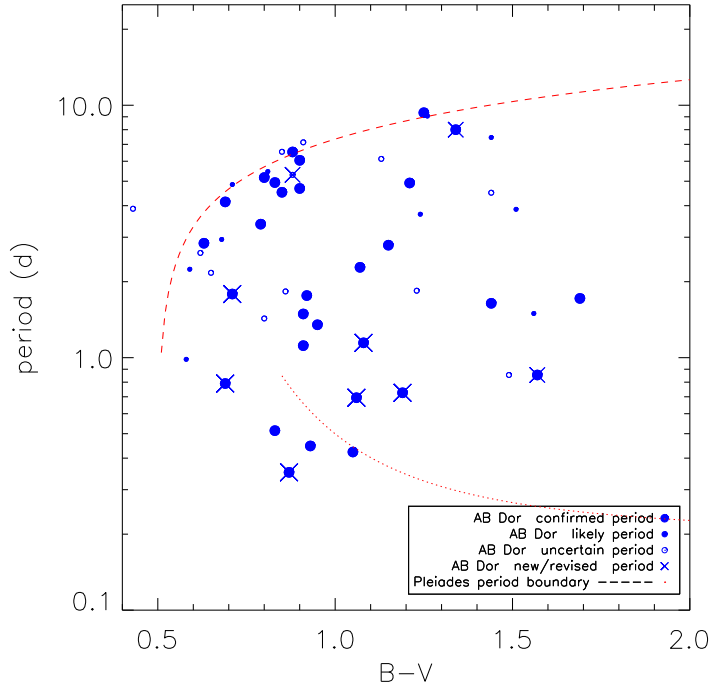

Fig. B.3 As in Fig. B.1 for AB Dor association.

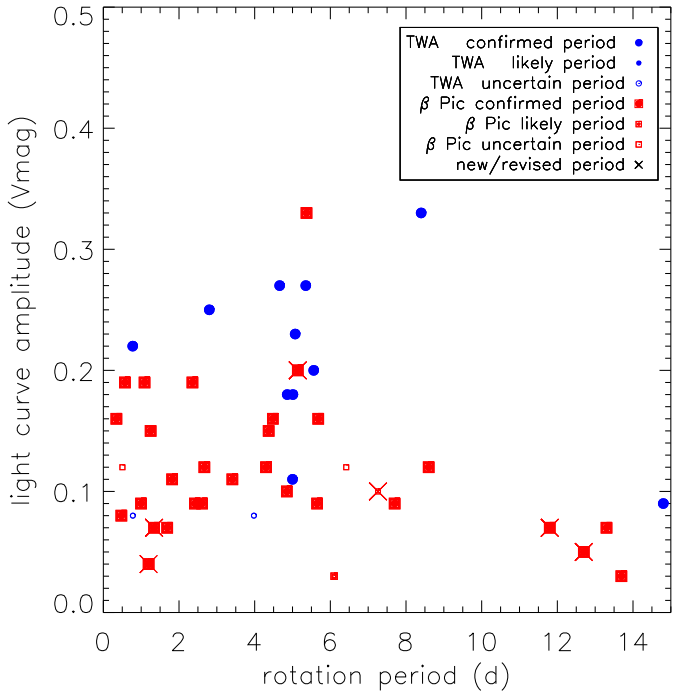

Fig. B.4 Distributions of light curve amplitudes in TWA + β Pic associations studied in Paper I.

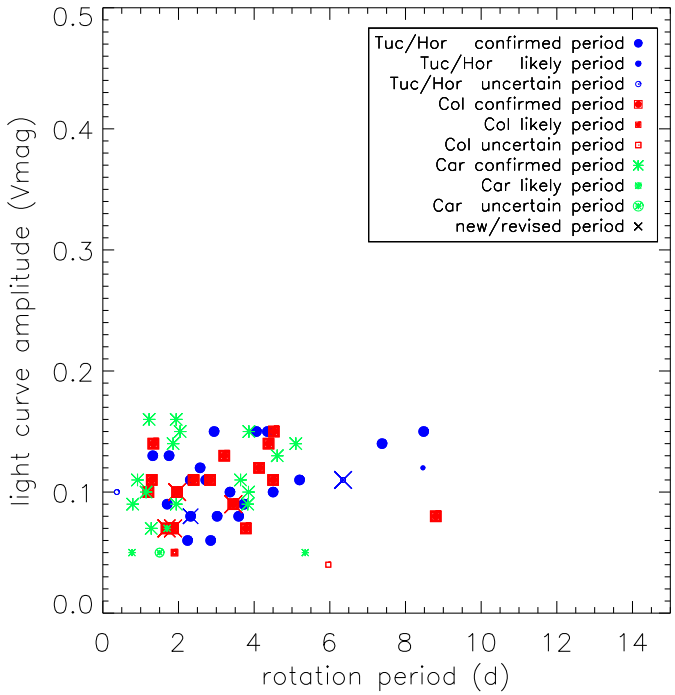

Fig. B.5 As in Fig. B.4 for Tuc/Hor + Car + Col associations.

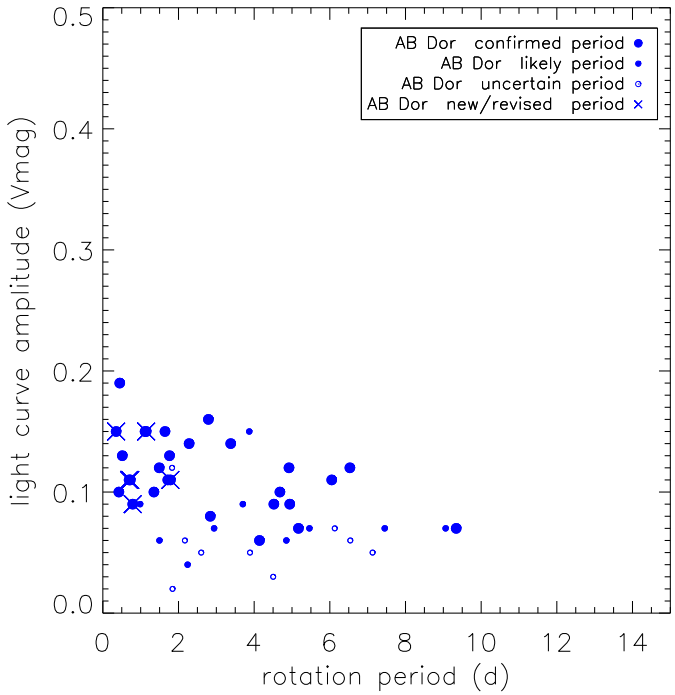

Fig. B.6 As in Fig. B.4 for AB Dor association.

Table B.2. Summary of period search based on ASAS/superWASP (SW) photometry.

Target	JD Initial	JD Final	Period (d)	ΔP (d)	Normalised Power	Power at 99% Confidence Level	note
			ϵ / η Chamaeleontis				
GSC 09235-01702	1871.8444	5039.5551	6.86	0.09	53.57	10.10	complete
GSC 09235-01702	1874.8509	1958.8509	6.8	0.2	9.23	6.56	
GSC 09235-01702	2623.7775	2709.7775	6.9	0.2	9.09	4.07	
GSC 09235-01702	2709.7775	2795.7775	6.8	0.2	7.36	4.43	
GSC 09235-01702	3034.8547	3110.8547	6.8	0.2	9.14	5.11	
GSC 09235-01702	3358.8184	3440.8184	6.8	0.2	7.74	5.43	
GSC 09235-01702	3440.8184	3522.8184	6.8	0.2	11.10	5.63	
GSC 09235-01702	3768.8445	3836.8445	6.8	0.3	7.66	4.92	
GSC 09235-01702	4175.7972	4258.7972	6.9	0.2	5.62	5.34	
GSC 09235-01702	4430.8545	4521.8545	6.8	0.2	4.79	4.41	
CD-69 1055	1877.8509	5069.5342	2.007	0.008	38.70	7.27	complete
CD-69 1055	2624.8184	2715.8184	1.97	0.02	5.55	4.61	
CD-69 1055	2715.8184	2806.8184	2.00	0.02	9.77	5.55	
CD-69 1055	3844.8540	3908.8540	2.01	0.02	5.56	4.85	
CD-69 1055	4105.8054	4189.8054	2.02	0.02	4.09	3.51	
CD-69 1055	4273.8054	4357.8054	1.99	0.02	7.58	4.79	
CD-69 1055	4436.8544	4531.8544	1.98	0.02	6.63	4.83	
CD-69 1055	4531.8544	4626.8544	1.99	0.02	14.18	5.49	
CD-69 1055	4626.8544	4721.8544	2.01	0.02	13.07	5.19	
CD-74 712	1871.8444	5072.5357	3.97	0.03	67.10	10.10	complete
CD-74 712	1874.8509	1963.8509	3.99	0.06	26.45	6.56	
CD-74 712	1963.8509	2052.8509	3.99	0.06	18.92	7.25	
CD-74 712	2052.8509	2141.8509	3.71	0.06	4.33	4.07	
CD-74 712	2442.5299	2525.4980	4.02	0.10	6.48	4.43	
CD-74 712	2623.7775	2714.7775	4.03	0.07	10.91	5.11	
CD-74 712	2714.7775	2805.7775	3.97	0.06	7.38	5.43	
CD-74 712	2805.7775	2896.7775	3.99	0.06	9.65	5.63	
CD-74 712	3035.8547	3112.8547	4.02	0.07	11.83	6.38	
CD-74 712	3112.8547	3189.8547	3.97	0.06	15.34	5.34	
CD-74 712	3356.8386	3447.8386	3.99	0.06	16.29	4.41	
CD-74 712	3447.8386	3538.8386	4.03	0.07	16.12	5.19	
CD-74 712	3538.8386	3629.8386	4.01	0.10	10.09	5.72	
CD-74 712	3704.8269	3772.8269	4.1	0.1	10.46	6.99	
CD-74 712	3772.8269	3840.8269	3.98	0.10	14.04	6.55	
CD-74 712	3840.8269	3908.8269	3.96	0.10	9.59	5.66	
CD-74 712	4180.7972	4268.7972	3.91	0.06	7.84	6.47	
CD-74 712	4268.7972	4356.7972	3.98	0.06	12.93	4.50	
CD-74 712	4430.8545	4527.8545	3.98	0.06	13.80	6.00	
CD-74 712	4527.8545	4624.8545	4.00	0.06	22.68	5.31	
CD-74 712	4624.8545	4721.8545	3.94	0.06	8.36	5.43	
CD-74 712	4794.8471	4885.8471	3.98	0.06	16.43	4.86	
CD-74 712	4885.8471	4976.8471	3.97	0.06	11.50	5.46	
CD-74 712	4976.8471	5067.8471	3.96	0.06	7.57	6.24	
CP-68 1388	1868.8585	5147.8586	3.56	0.03	90.71	8.66	complete
CP-68 1388	1873.8054	1949.8054	3.59	0.05	15.45	4.79	
CP-68 1388	2623.7356	2701.7356	3.58	0.05	11.01	4.29	
CP-68 1388	2701.7356	2779.7356	3.56	0.05	11.69	5.97	
CP-68 1388	3011.8778	3098.8778	3.56	0.05	11.99	4.88	
CP-68 1388	3098.8778	3185.8778	3.58	0.05	9.68	5.22	

Table B.2 (cont'd)

Target	JD Initial	JD Final	Period (d)	ΔP (d)	Normalised Power	Power at 99% Confidence Level	note
CP-68 1388	3434.8359	3512.8359	3.59	0.05	11.08	7.13	
CP-68 1388	3739.8750	3821.8750	3.58	0.05	10.66	5.71	
CP-68 1388	3821.8750	3903.8750	3.56	0.05	11.72	4.56	
CP-68 1388	4105.7609	4174.7609	3.52	0.08	8.77	4.14	
CP-68 1388	4174.7609	4243.7609	3.54	0.08	6.43	4.74	
CP-68 1388	4485.8798	4583.8798	3.64	0.05	7.45	5.03	
CP-68 1388	4583.8798	4681.8798	3.59	0.05	8.63	4.87	
GSC 9419-01065	1869.8563	5037.5285	8.0	0.1	67.51	6.34	complete
GSC 9419-01065	3043.8461	3114.8461	8.1	0.3	6.15	5.05	
GSC 9419-01065	4431.8295	4520.8295	8.0	0.3	6.46	5.07	
GSC 9419-01065	4520.8295	4609.8295	7.9	0.3	10.95	5.35	
GSC 9419-01065	4609.8295	4698.8295	7.9	0.3	8.45	3.97	
GSC 9239-1495	1871.8444	5064.5336	1.676	0.006	8.61	7.28	complete
GSC 9239-1495	2623.7775	2881.7775	1.688	0.006	6.46	5.59	
GSC 9239-1495	3356.8386	3605.8386	1.668	0.006	5.48	4.88	
GSC 9239-1495	4794.8471	5046.8471	1.680	0.006	4.96	3.56	
GSC 9239-1572	1874.8509	2141.8509	1.536	0.005	30.46	4.14	
GSC 9239-1572	2442.5299	2525.4980	1.53	0.01	7.41	3.95	
GSC 9239-1572	2623.7775	2881.7775	1.536	0.005	17.13	5.57	
GSC 9239-1572	2958.8547	3188.8547	1.536	0.005	20.58	6.17	
GSC 9239-1572	3356.8386	3605.8386	1.532	0.005	9.08	5.93	
GSC 9239-1572	3704.8269	3906.8269	1.540	0.005	11.94	4.77	
GSC 9239-1572	4092.7972	4358.7972	1.536	0.005	10.35	4.98	
GSC 9239-1572	4430.8545	4723.8545	1.536	0.005	11.88	4.05	
GSC 9239-1572	4794.8471	5067.8471	1.556	0.005	4.74	4.05	
GSC 9416-1029	3358.8226	3605.8226	5.53	0.06	5.04	4.04	
GSC 9416-1029	3676.8682	3911.8682	5.50	0.06	4.31	4.04	
GSC 9420-0948	1869.8563	5037.5285	4.45	0.04	130.1	7.20	complete
GSC 9420-0948	2623.7915	2707.7915	4.46	0.08	8.16	4.56	
GSC 9420-0948	2707.7915	2791.7915	4.44	0.08	13.39	6.70	
GSC 9420-0948	3043.8461	3114.8461	4.42	0.08	9.65	5.62	
GSC 9420-0948	3358.8226	3440.8226	4.45	0.08	7.42	4.63	
GSC 9420-0948	3440.8226	3522.8226	4.44	0.08	13.62	5.64	
GSC 9420-0948	3754.8682	3832.8682	4.45	0.08	11.82	5.15	
GSC 9420-0948	3832.8682	3910.8682	4.5	0.1	8.57	4.59	
GSC 9420-0948	4256.7947	4338.7947	4.5	0.1	5.32	5.01	
GSC 9420-0948	4431.8295	4521.8295	4.53	0.08	5.13	3.80	
GSC 9420-0948	4521.8295	4611.8295	4.41	0.08	8.62	5.61	
GSC 9420-0948	4611.8295	4701.8295	4.50	0.08	7.12	5.26	
HD 104467	1869.8563	5037.5285	4.43	0.04	18.02	9.51	complete
HD 104467	2707.7915	2791.7915	4.39	0.08	9.38	6.12	
HD 104467	3043.8461	3114.8461	4.41	0.08	5.90	5.24	
HD 104467	3775.8292	3843.8292	4.6	0.1	7.02	5.53	
HD 104467	3843.8292	3911.8292	4.4	0.1	5.37	3.18	
HD 105923	1871.8444	5039.5551	5.05	0.05	17.22	7.27	complete
HD 105923	1874.8509	1958.8509	5.3	0.1	10.65	5.49	
HD 105923	1958.8509	2042.8509	5.1	0.1	8.71	6.32	
HD 105923	2623.7775	2709.7775	5.0	0.2	5.27	4.83	
HD 105923	2709.7775	2795.7775	5.2	0.1	12.52	5.43	
HD 105923	3110.8547	3186.8547	5.0	0.1	4.74	4.00	
HD 105923	3771.8269	3838.8269	5.0	0.2	8.28	4.20	
HD 105923	4092.7972	4175.7972	5.0	0.2	3.93	3.39	

Table B.2 (cont'd)

Target	JD Initial	JD Final	Period (d)	ΔP (d)	Normalised Power	Power at 99% Confidence Level	note
HD 105923	4175.7972	4258.7972	5.1	0.1	6.40	4.74	
HD 105923	4430.8545	4521.8545	5.1	0.1	7.25	3.78	
HD 105923	4521.8545	4612.8545	5.2	0.1	10.58	7.52	
HD 105923	4612.8545	4703.8545	5.2	0.1	10.47	6.63	
HIP 58490	1869.8563	5039.5551	8.0	0.1	56.42	6.45	complete
HIP 58490	2623.7915	2707.7915	8.1	0.3	9.79	5.02	
HIP 58490	2707.7915	2791.7915	8.1	0.3	10.29	4.52	
HIP 58490	3043.8461	3114.8461	8.0	0.3	9.73	5.16	
HIP 58490	3440.8184	3522.8184	7.9	0.3	7.44	5.85	
HIP 58490	3771.8269	3838.8269	8.0	0.4	9.64	5.18	
HIP 58490	4430.8545	4521.8545	8.1	0.3	5.68	4.58	
HIP 58490	4612.8545	4703.8545	8.0	0.3	6.95	5.51	
TYC 9246-971-1	1877.8509	5069.5342	3.75	0.03	24.47	6.97	complete
TYC 9246-971-1	1886.8366	1971.8366	3.74	0.06	12.29	4.19	
TYC 9246-971-1	3047.8403	3117.8403	3.69	0.08	6.47	4.60	
TYC 9246-971-1	3356.8386	3447.8386	3.78	0.06	7.12	4.65	
TYC 9246-971-1	3447.8386	3538.8386	3.71	0.06	7.81	7.11	
TYC 9246-971-1	3538.8386	3629.8386	3.73	0.06	5.79	4.91	
TYC 9246-971-1	3844.8540	3908.8540	3.73	0.09	6.26	4.27	
TYC 9246-971-1	4179.8378	4268.8378	3.67	0.05	5.02	4.99	
TYC 9246-971-1	4268.8378	4357.8378	3.70	0.06	6.99	5.89	
TYC 9246-971-1	4436.8544	4531.8544	3.69	0.06	6.54	4.73	
HD 58285	3358.8226	3440.8226	3.24	0.06	4.86	4.09	
RECX 1	1868.7819	5137.7883	4.50	0.04	71.19	7.30	complete
RECX 1	1871.7871	2000.7871	4.35	0.08	19.00	5.97	
RECX 1	2129.7871	2258.7871	4.49	0.08	6.56	4.22	
RECX 1	2441.5036	2689.5036	4.5	0.2	7.24	7.06	
RECX 1	2689.5036	2937.5036	4.5	0.2	15.72	5.98	
RECX 1	2937.5036	3185.5036	4.48	0.04	21.39	6.05	
RECX 1	3488.7719	3554.7719	4.4	0.1	6.47	5.08	
RECX 1	3622.8964	3716.8964	4.40	0.08	8.04	6.08	
RECX 1	3716.8964	3810.8964	4.41	0.08	21.55	5.06	
RECX 1	3810.8964	3904.8964	4.59	0.09	13.26	5.67	
RECX 1	4091.7670	4437.7670	4.5	0.2	40.27	7.02	
RECX 1	4437.7670	4783.7670	4.50	0.04	33.98	8.17	
RECX 1	4783.7670	5129.7670	4.37	0.04	15.89	4.85	
RECX 4	1868.7819	5137.7883	7.1	0.4	70.37	7.77	complete
RECX 4	1871.7871	1998.7871	7.2	0.2	19.97	5.70	
RECX 4	2937.5036	3185.5036	7.2	0.1	10.97	6.03	
RECX 4	3356.7719	3539.7719	7.2	0.1	19.64	5.59	
RECX 4	4091.7670	4437.7670	7.1	0.1	14.58	6.72	
RECX 4	4437.7670	4783.7670	7.1	0.1	21.54	8.10	
RECX 4	4783.7670	5129.7670	7.1	0.1	10.51	9.22	
RECX 10	1868.7819	5137.7883	20.1	3.3	22.60	7.23	complete
RECX 10	1871.7871	1998.7871	20.3	1.7	22.19	5.64	
RECX 10	2937.5036	3185.5036	20.4	0.8	11.55	5.42	
RECX 10	3356.7719	3539.7719	20.0	0.8	6.31	6.12	
RECX 10	4437.7670	4783.7670	20.8	0.9	18.30	6.42	
RECX 10	4783.7670	5129.7670	20.6	0.9	7.30	5.49	
RECX 11	1868.7819	5137.7883	4.84	0.05	41.35	7.55	complete
RECX 11	2129.7871	2258.7871	4.81	0.09	8.71	4.39	
RECX 11	2441.5036	2689.5036	4.86	0.05	15.58	6.60	

Table B.2 (cont'd)

Target	JD Initial	JD Final	Period (d)	ΔP (d)	Normalised Power	Power at 99% Confidence Level	note
RECX 11	2937.5036	3185.5036	4.81	0.05	11.84	7.28	
RECX 11	3356.7719	3539.7719	4.79	0.05	18.58	6.02	
RECX 11	4091.7670	4437.7670	4.84	0.05	13.03	8.04	
RECX 11	4437.7670	4783.7670	4.74	0.05	10.80	6.04	
RECX 11	4783.7670	5129.7670	4.85	0.05	19.77	7.24	
RECX 12	1871.7871	2000.7871	1.261	0.006	7.73	7.69	
RECX 12	2129.7871	2258.7871	1.257	0.006	4.91	4.30	
			Octans				
CD-47 1999	2920.8874	3131.8874	1.265	0.003	12.53	5.78	
CD-47 1999	3680.9338	3784.9338	1.269	0.006	9.46	6.23	
CD-47 1999	3784.9338	3888.9338	1.265	0.006	7.14	5.90	
CD-58 860	1868.6697	4879.5959	2.61	0.01	17.06	7.80	complete
CD-58 860	2445.9293	2671.9293	2.61	0.01	10.20	4.90	
CD-58 860	2897.9293	3123.9293	2.61	0.01	14.76	6.76	
CD-58 860	3357.6559	3539.6559	2.61	0.06	8.34	5.59	
CD-58 860	3539.6559	3721.6559	2.62	0.01	10.10	7.32	
CD-58 860	3721.6559	3903.6559	2.62	0.06	15.06	5.67	
CD-58 860	4292.9307	4486.9307	2.62	0.01	20.18	5.82	
CD-58 860	4486.9307	4680.9307	2.62	0.06	10.56	6.31	
CD-58 860	4680.9307	4874.9307	2.61	0.01	9.27	5.94	
CD-66 395	1871.7637	1951.7637	0.3713	0.0006	11.97	6.97	
CD-66 395	1951.7637	2031.7637	0.3713	0.0008	6.69	4.23	
CD-66 395	2186.9190	2255.9190	0.3713	0.0008	21.62	4.80	
CD-66 395	2687.4489	2930.4489	0.3713	0.0005	30.37	5.27	
CD-66 395	3574.9351	3684.9351	0.3713	0.0006	11.59	4.49	
CD-66 395	3684.9351	3794.9351	0.3713	0.0006	17.34	6.16	
CD-72 248	1876.6882	1953.6882	0.2357	0.0002	6.43	4.14	
CD-72 248	2186.8899	2255.8899	0.2357	0.0003	7.73	6.95	
CD-72 248	2466.9251	2687.9251	0.2516	0.0001	10.31	5.52	
CD-72 248	3433.6240	3510.6240	0.2357	0.0003	7.09	5.29	
CD-72 248	4362.6561	4619.6561	0.2357	0.0001	6.59	5.41	
CD-72 248	4619.6561	4876.6561	0.2357	0.0001	6.93	6.47	
CD-87 121	2000.5296	2127.5296	0.762	0.001	7.99	5.92	
CD-87 121	2127.5296	2254.5296	0.762	0.001	6.86	5.69	
CD-87 121	2440.8676	2673.8676	0.762	0.001	13.14	5.96	
CD-87 121	4433.5303	4781.5303	0.766	0.001	7.53	5.14	
CP-79 1037	2052.9009	2142.9009	1.95	0.02	8.60	5.69	
CP-79 1037	2142.9009	2232.9009	1.93	0.02	4.79	4.74	
CP-79 1037	4246.8967	4341.8967	1.97	0.02	6.32	5.49	
CP-79 1037	4341.8967	4436.8967	2.00	0.02	7.56	5.34	
CP-79 1037	4616.8960	4714.8960	1.99	0.02	6.61	5.21	
CP-82 784	1873.5198	5122.6208	1.373	0.004	13.51	9.18	complete
CP-82 784	2005.5197	2132.5197	1.365	0.007	7.49	5.43	
CP-82 784	2132.5197	2259.5197	1.377	0.008	15.16	4.44	
CP-82 784	2440.7945	2529.7945	1.373	0.008	8.42	4.78	
CP-82 784	2678.8605	2778.8605	1.381	0.008	14.19	6.05	
CP-82 784	3357.5451	3542.5451	1.377	0.007	10.11	4.43	
CP-82 784	3542.5451	3727.5451	1.377	0.004	17.83	5.43	
CP-82 784	4088.5782	4426.5782	1.365	0.004	7.38	5.17	
CP-82 784	4426.5782	4764.5782	1.369	0.004	28.52	8.10	

Table B.2 (cont'd)

Target	JD Initial	JD Final	Period (d)	ΔP (d)	Normalised Power	Power at 99% Confidence Level	note
CP-82 784	4764.5782	5102.5782	1.373	0.004	7.51	7.30	
HD 274576	1868.7042	4881.6720	2.211	0.010	19.20	8.96	complete
HD 274576	1872.7055	1951.7055	2.22	0.02	16.54	4.56	
HD 274576	2182.9337	2267.9337	2.20	0.02	10.95	5.31	
HD 274576	3038.9243	3141.9243	2.26	0.02	5.57	4.00	
HD 274576	3355.8336	3432.8336	2.20	0.02	5.16	4.85	
HD 274576	3432.8336	3509.8336	2.25	0.03	6.82	4.19	
HD 274576	3670.9228	3768.9228	2.20	0.02	10.02	4.72	
HD 274576	3768.9228	3866.9228	2.21	0.02	11.46	4.47	
HD 274576	4298.9278	4398.9278	2.13	0.02	5.12	4.47	
HD 274576	4498.9278	4598.9278	2.27	0.02	7.93	5.98	
HD 274576	3993.4992	4143.3347	2.203	0.009	114.96	12.63	SW complete
HD 274576	3997.4978	4067.4978	2.203	0.029	70.67	5.31	SW
HD 274576	4067.4978	4137.4978	2.227	0.030	74.87	6.89	SW
TYC 7066 1037 1	1872.7432	1948.7432	2.47	0.04	8.00	5.51	
TYC 7066 1037 1	3033.9411	3129.9411	2.49	0.03	5.53	4.62	
TYC 7066 1037 1	4302.9385	4403.9385	2.55	0.03	5.93	3.58	
TYC 7066 1037 1	3860.2139	4531.3053	2.47	0.01	37.63	6.81	SW complete
TYC 7066 1037 1	4023.4705	4096.4705	2.46	0.03	34.48	5.57	SW
TYC 7066 1037 1	4096.4705	4169.4705	2.47	0.03	51.76	5.93	SW
TYC 7066 1037 1	4457.4888	4528.4888	2.47	0.02	58.43	8.76	SW
TYC 9300 0529 1	2140.8624	2232.8624	2.55	0.03	5.59	5.20	
TYC 9300 0529 1	2872.8894	2965.8894	2.58	0.03	5.61	4.63	
TYC 9300 0529 1	4329.8784	4427.8784	2.59	0.03	4.27	3.48	
TYC 9300 0529 1	4498.8823	4593.8823	2.53	0.03	3.71	3.61	
			Argus / IC 2391				
HD 5578	2756.9237	3058.9237	1.461	0.004	9.14	7.65	
HD 5578	3512.9127	3787.9127	1.465	0.004	8.81	8.01	
HD 5578	4232.9203	4514.9203	1.461	0.004	9.00	6.77	
HD 5578	4597.9214	4879.9214	1.465	0.004	14.47	7.55	
CD-28 3434	1868.7473	5162.7932	3.82	0.03	48.14	7.58	complete
CD-28 3434	1871.7499	1996.7499	3.83	0.06	19.23	6.81	
CD-28 3434	2116.9412	2253.9412	3.82	0.06	13.09	8.32	
CD-28 3434	2860.9165	3161.9165	3.83	0.03	12.87	6.95	
CD-28 3434	3356.6886	3526.6886	4.11	0.03	6.77	5.52	
CD-28 3434	3621.8928	3889.8928	3.83	0.03	14.68	6.42	
CD-28 3434	4333.9137	4621.9137	3.83	0.03	12.27	7.53	
CD-28 3434	4701.9195	4958.9195	3.82	0.03	15.31	7.57	
CD-28 3434	4105.3081	4531.3064	3.81	0.02	146.95	8.21	SW complete
CD-28 3434	4109.3072	4170.3917	3.88	0.09	67.73	4.76	SW
CD-28 3434	4386.4985	4457.4985	3.82	0.05	110.47	5.12	SW
CD-28 3434	4457.4985	4528.4985	3.80	0.05	73.42	5.88	SW
CD-39 5883	2546.8786	2841.8786	4.05	0.03	8.08	6.30	
CD-39 5883	3644.8916	3905.8916	4.23	0.04	6.83	6.35	
CD-39 5883	3860.2194	4604.3476	4.05	0.03	146.95	7.57	SW complete
CD-39 5883	3863.2394	3906.2779	4.24	0.11	19.68	4.94	SW
CD-39 5883	4089.4374	4163.4374	4.01	0.09	79.01	6.58	SW
CD-39 5883	4163.4374	4237.4374	4.05	0.06	68.37	5.76	SW
CD-39 5883	4454.4383	4528.4383	4.26	0.07	62.94	7.56	SW
CD-39 5883	4528.4383	4602.4383	4.18	0.10	75.44	6.20	SW

Table B.2 (cont'd)

Target	JD Initial	JD Final	Period (d)	ΔP (d)	Normalised Power	Power at 99% Confidence Level	note
CD-42 2906	1868.7513	5158.7728	3.95	0.06	19.56	7.52	complete
CD-42 2906	1871.8279	2055.8279	3.97	0.06	33.79	7.18	
CD-42 2906	2129.9308	2255.9308	4.01	0.07	10.87	9.24	
CD-42 2906	2497.9017	3173.9017	3.98	0.03	22.81	10.04	
CD-42 2906	3359.7081	3902.7081	3.95	0.03	39.04	6.63	
CD-43 3604	1873.8370	2067.8370	0.890	0.002	9.16	5.71	
CD-43 3604	2878.9207	3175.9207	0.890	0.002	19.32	5.42	
CD-43 3604	3357.7552	3545.7552	0.890	0.002	15.49	9.34	
CD-43 3604	4332.9224	4641.9224	0.890	0.002	10.58	6.46	
CD-48 2972	1871.8345	2067.8345	1.038	0.004	25.39	9.74	
CD-48 2972	2132.9285	2256.9285	1.030	0.004	10.06	5.35	
CD-48 2972	3620.9080	3905.9080	1.038	0.002	11.58	6.29	
CD-48 2972	4092.6961	4276.6961	1.030	0.002	6.41	4.84	
CD-48 2972	4333.9123	4641.9123	1.030	0.002	6.28	5.26	
CD-48 2972	4701.9178	4943.9178	1.026	0.002	7.93	5.99	
CD-48 3199	1868.7772	5161.8149	2.191	0.010	20.06	9.22	complete
CD-48 3199	1871.8345	2067.8345	2.18	0.02	9.42	5.54	
CD-48 3199	2132.9285	2256.9285	2.20	0.02	6.97	4.57	
CD-48 3199	2497.9271	3173.9271	2.191	0.010	15.35	8.06	
CD-48 3199	3334.7985	3542.7985	2.195	0.010	11.61	5.74	
CD-48 3199	3620.9080	3905.9080	2.191	0.010	14.15	7.72	
CD-48 3199	4333.9123	4943.9123	2.187	0.010	11.08	7.14	
CD-52 9381	1873.5259	5084.7841	5.18	0.05	37.03	7.06	complete
CD-52 9381	1981.8680	2232.8680	5.18	0.05	29.98	7.21	
CD-52 9381	2599.7286	2755.7286	5.1	0.2	8.07	5.31	
CD-52 9381	2697.8917	2981.8917	5.19	0.05	18.91	8.02	
CD-52 9381	3076.8905	3193.8905	5.1	0.1	10.72	4.85	
CD-52 9381	4168.8927	4438.8927	5.22	0.06	6.62	5.92	
CD-52 9381	4548.8800	4803.8800	5.12	0.05	19.86	5.09	
CD-56 1438	1872.7514	2054.7514	0.2436	0.0002	12.11	6.66	
CD-57 2315	1868.8053	5137.8208	2.099	0.009	10.94	8.80	complete
CD-58 2194	1868.8053	5137.8208	5.16	0.05	10.00	7.90	complete
CD-58 2194	1872.7631	2079.7631	5.33	0.06	9.95	5.73	
CD-58 2194	2546.8499	2828.8499	5.16	0.05	6.20	5.69	
CD-58 2194	3622.9120	3906.9120	5.21	0.05	10.05	6.88	
CD-58 2194	4091.7565	4967.7565	4.91	0.05	13.28	6.67	
CPD-62 1197	1872.8598	2083.8598	1.253	0.003	13.02	5.95	
CPD-62 1197	2558.8324	2834.8324	1.249	0.003	21.06	5.09	
CPD-62 1197	3358.7779	3562.7779	1.265	0.003	7.00	6.27	
CPD-62 1197	3632.8886	3906.8886	1.249	0.003	12.14	5.32	
CPD-62 1197	4090.7246	4298.7246	1.253	0.003	9.02	5.11	
CPD-62 1197	4351.9091	4664.9091	1.261	0.003	13.65	8.29	
CPD-62 1197	4730.8828	4915.8828	1.261	0.003	10.24	6.31	
CD-65 817	1868.8405	5125.8485	2.74	0.02	18.20	9.15	complete
CD-65 817	2566.8599	3184.8599	2.73	0.02	11.57	8.37	
CD-65 817	3357.8059	3572.8059	2.73	0.02	8.74	7.35	
CD-65 817	3654.8687	3906.8687	2.75	0.02	7.82	5.27	
CD-65 817	4374.8949	4665.8949	2.75	0.02	7.82	6.00	
CD-74 673	1869.8563	5072.5357	3.48	0.02	19.27	8.29	complete
CD-74 673	1874.8487	2141.8487	3.48	0.02	10.66	7.07	
CD-74 673	2623.7845	2877.7845	3.49	0.02	12.29	7.15	
CD-74 673	3356.8386	3629.8386	3.53	0.03	26.55	8.20	

Table B.2 (cont'd)

Target	JD Initial	JD Final	Period (d)	ΔP (d)	Normalised Power	Power at 99% Confidence Level	note
CD-74 673	4092.7972	4358.7972	3.47	0.02	22.71	6.86	
CD-74 673	4430.8545	4707.8545	3.49	0.02	34.33	8.11	
CD-74 673	4794.8471	5067.8471	3.47	0.02	10.96	6.49	
CD-75 652	1885.8485	5088.5260	2.27	0.01	20.07	11.83	complete
CD-75 652	1888.8541	2171.8541	2.36	0.01	15.17	6.97	
CD-75 652	2441.5455	2543.5455	2.29	0.02	5.57	4.53	
CD-75 652	2624.8491	2909.8491	2.29	0.01	10.75	6.29	
CD-75 652	2987.8514	3183.8514	2.30	0.01	9.39	6.12	
CD-75 652	3356.8386	3648.8386	2.27	0.01	34.25	5.67	
CD-75 652	3716.8540	3911.8540	2.27	0.01	26.66	6.39	
CD-75 652	4105.8054	4378.8054	2.26	0.01	9.08	6.82	
CD-75 652	4436.8544	4741.8544	2.27	0.01	29.56	6.20	
CD-75 652	4809.8432	5085.8432	2.28	0.01	18.77	5.82	
CP-69 1432	2924.8778	3185.8778	1.030	0.002	16.69	6.51	
CP-69 1432	3657.8750	3905.8750	1.030	0.002	17.12	6.06	
CP-69 1432	4091.7762	4314.7762	1.030	0.002	6.71	6.36	
HD 309851	1868.8405	5125.8485	1.816	0.007	18.96	10.05	complete
HD 309851	1873.8054	2103.8054	1.820	0.007	28.43	6.73	
HD 309851	2541.8851	3187.8851	1.816	0.007	29.06	6.98	
HD 309851	3357.8059	3572.8059	1.816	0.007	8.28	6.80	
HD 309851	4091.7744	4303.7744	1.820	0.007	9.72	5.46	
HD 309851	4374.8949	4665.8949	1.812	0.007	11.68	7.93	
HD 310316	1868.8585	5049.4895	3.61	0.03	15.30	8.99	complete
HD 310316	1873.8054	2102.8054	3.61	0.03	13.70	5.45	
HD 310316	2200.8578	2254.7702	3.5	0.1	5.09	3.26	
HD 310316	2924.8778	3185.8778	3.64	0.03	16.06	5.35	
HD 310316	3657.8750	3905.8750	3.64	0.03	16.06	6.55	
HD 84075	1870.7871	5113.8750	2.49	0.01	9.92	9.23	complete
HD 84075	2168.8916	2258.8916	2.44	0.02	8.05	6.36	
HD 85151A	1868.8364	5023.4946	0.998	0.002	48.08	7.72	complete
HD 85151A	2913.8875	3187.8875	0.994	0.002	6.08	5.90	
HD 85151A	4365.9008	4672.9008	0.994	0.002	9.03	6.36	
HD 85151A	3863.2395	3906.2782	0.969	0.007	13.81	3.24	SW complete
HD 85151A	4089.4370	4163.4370	0.969	0.005	44.50	5.06	SW
HD 85151A	4454.4380	4527.4380	0.973	0.003	17.17	6.73	SW
HD 85151A	4527.4380	4600.4380	0.965	0.005	16.56	4.86	SW
HD 133813	1903.8423	5099.5151	4.09	0.03	22.25	6.81	complete
HD 133813	1906.8555	2187.8555	4.10	0.03	23.58	5.73	
HD 133813	2566.5620	2691.5620	4.01	0.10	6.02	4.03	
HD 133813	2625.8517	2931.8517	4.04	0.03	12.64	8.39	
HD 133813	2996.8513	3188.8513	4.10	0.03	22.09	4.87	
HD 133813	3727.8559	3911.8559	4.08	0.03	20.24	4.92	
HD 133813	4105.8605	4387.8605	4.09	0.03	12.50	5.86	
HD 133813	4463.8555	4760.8555	4.10	0.03	23.67	6.04	
HD 133813	4822.8563	5090.8563	4.11	0.03	20.77	6.19	
PMM 1083	1868.8053	5137.8208	1.333	0.004	56.55	8.22	complete
PMM 1083	1872.7631	2079.7631	1.333	0.004	12.38	5.67	
PMM 1083	2168.8629	2257.7139	1.329	0.007	9.77	8.97	
PMM 1083	2546.8298	2828.8298	1.333	0.004	17.04	7.00	
PMM 1083	2886.9180	3184.9180	1.333	0.004	16.35	7.20	
PMM 1083	3358.7697	3559.7697	1.333	0.004	11.43	6.28	
PMM 1083	3622.9120	3906.9120	1.333	0.004	12.76	7.41	

Table B.2 (cont'd)

Target	JD Initial	JD Final	Period (d)	ΔP (d)	Normalised Power	Power at 99% Confidence Level	note
PMM 1083	4091.7565	4659.7565	1.333	0.004	9.89	7.65	
PMM 1083	4728.9038	4967.9038	1.333	0.004	11.59	8.78	
PMM 1142	1868.8053	5137.8208	0.998	0.002	26.90	10.42	complete
PMM 1373	1869.7983	5137.8208	5.38	0.06	14.97	8.65	complete
PMM 1373	1874.7488	2079.7488	5.33	0.06	7.16	4.99	
PMM 1560	1868.8053	5145.8070	0.998	0.002	9.82	6.97	complete
PMM 1759	3358.7697	3556.7697	16.6	0.6	5.84	5.46	
PMM 1820	1872.7631	2079.7631	0.5269	0.0006	7.24	4.82	
PMM 1820	2546.8298	2828.8298	0.5269	0.0006	13.09	4.91	
PMM 1820	3358.7697	3559.7697	0.5269	0.0006	6.21	6.09	
PMM 1820	3622.9120	3906.9120	0.5269	0.0006	8.94	6.67	
PMM 2012	2173.8772	2257.7139	2.21	0.02	7.88	6.09	
PMM 2012	2886.9180	3184.9180	2.211	0.010	5.90	5.13	
PMM 2012	4091.7565	4659.7565	2.207	0.010	9.39	8.15	
PMM 2012	4728.9038	4967.9038	2.211	0.010	11.13	5.10	
PMM 2182	1872.7631	2079.7631	1.437	0.004	17.76	4.87	
PMM 2182	2173.8772	2257.7139	1.469	0.009	7.89	4.27	
PMM 2182	2553.8315	2828.8315	1.437	0.004	11.00	7.69	
PMM 2182	3358.7697	3559.7697	1.465	0.004	5.87	5.38	
PMM 2182	3622.9120	3906.9120	1.473	0.004	7.97	7.30	
PMM 2182	4090.7318	4659.7318	1.473	0.004	9.89	7.13	
PMM 2182	4728.9038	4967.9038	1.437	0.004	12.90	7.21	
PMM 2456	1872.7631	2079.7631	1.030	0.002	17.07	6.51	
PMM 3359	1868.8053	5145.8365	3.84	0.03	9.56	7.34	complete
PMM 3359	1872.7631	2079.7631	3.84	0.03	11.68	5.08	
PMM 3359	2168.8629	2257.7139	3.82	0.06	6.93	5.78	
PMM 3359	2546.8298	2828.8298	4.01	0.03	9.04	5.45	
PMM 3359	2886.9180	3184.9180	3.94	0.03	5.19	5.05	
PMM 3359	3622.9120	3906.9120	3.85	0.03	9.75	6.72	
PMM 3359	4090.7318	4659.7318	4.03	0.03	16.07	9.54	
PMM 351	1868.8053	5137.8208	1.931	0.007	11.61	7.89	complete
PMM 351	1872.7631	2079.7631	1.923	0.007	8.05	6.80	
PMM 351	2168.8629	2257.7139	1.94	0.02	9.30	4.36	
PMM 351	2546.8298	2828.8298	1.999	0.008	9.20	6.05	
PMM 351	2886.9180	3184.9180	1.999	0.008	8.67	7.78	
PMM 351	3622.9120	3906.9120	1.931	0.007	8.29	6.13	
PMM 351	4091.7565	4967.7565	1.931	0.007	21.56	8.08	
PMM 3695	1868.8053	4948.6174	0.223	0.004	9.59	9.50	complete
PMM 4280	4723.8939	4967.8939	17.0	0.6	4.59	4.35	
PMM 4336	1868.8053	5145.8365	3.71	0.03	11.71	6.54	complete
PMM 4336	1872.7631	2079.7631	3.72	0.03	11.73	6.70	
PMM 4336	2546.8298	2828.8298	3.67	0.03	8.91	7.69	
PMM 4336	4364.8733	4659.8733	3.70	0.03	9.59	5.01	
PMM 4336	4745.8821	4967.8821	3.69	0.03	7.61	4.97	
PMM 4362	1868.8053	5145.8365	3.93	0.03	14.39	6.79	complete
PMM 4362	1872.7631	2079.7631	3.91	0.03	13.14	4.78	
PMM 4362	2546.8298	2828.8298	3.92	0.02	6.32	5.57	
PMM 4362	2886.9180	3184.9180	3.92	0.03	9.05	5.09	
PMM 4362	3359.7666	3559.7666	3.90	0.03	7.28	5.50	
PMM 4413	1868.8053	5145.8365	5.05	0.05	18.15	7.75	complete
PMM 4413	1872.7631	2079.7631	5.08	0.05	8.49	5.19	
PMM 4413	2546.8298	2828.8298	5.09	0.05	6.59	5.11	

Table B.2 (cont'd)

Target	JD Initial	JD Final	Period (d)	ΔP (d)	Normalised Power	Power at 99% Confidence Level	note
PMM 4413	3631.8528	3906.8528	5.05	0.05	13.36	5.86	
PMM 4467	1868.8053	5145.8365	3.85	0.03	34.75	8.92	complete
PMM 4467	2168.8629	2257.7139	3.89	0.06	6.38	5.29	
PMM 4467	2546.8298	2828.8298	3.84	0.03	10.35	5.80	
PMM 4467	2886.9180	3184.9180	3.85	0.03	10.08	6.90	
PMM 4467	3359.7666	3559.7666	3.85	0.03	9.48	5.78	
PMM 4467	4090.7318	4298.7318	3.87	0.03	5.99	5.29	
PMM 4467	4351.9129	4659.9129	3.85	0.03	13.37	6.28	
PMM 4467	4745.8821	4967.8821	3.847	0.004	16.97	7.42	
PMM 4636	1872.7631	2079.7631	0.834	0.003	5.90	4.59	
PMM 4809	1868.8053	5145.8365	2.60	0.01	15.29	7.05	complete
PMM 4809	1872.7631	2079.7631	2.60	0.01	12.51	5.03	
PMM 4809	2886.9180	3184.9180	2.61	0.01	11.78	10.81	
PMM 4809	3359.7666	3559.7666	2.60	0.01	16.76	5.17	
PMM 4809	4090.7318	4298.7318	2.61	0.01	17.99	7.31	
PMM 4809	4351.9129	4659.9129	2.60	0.01	11.52	7.07	
PMM 4809	4745.8821	4967.8821	2.68	0.01	8.47	7.39	
PMM 4902	2546.8298	2828.8298	4.82	0.05	7.48	6.00	
PMM 4902	2886.9180	3184.9180	5.10	0.05	6.47	5.80	
PMM 4902	4090.7318	4298.7318	4.98	0.05	6.86	5.54	
PMM 5376	1868.8053	4907.7022	7.162	0.003	7.33	6.20	complete
PMM 5884	1868.8053	5137.8545	3.03	0.02	20.49	8.45	complete
PMM 5884	2173.8772	2257.7139	3.12	0.04	9.14	5.57	
PMM 5884	2546.8399	2828.8399	3.04	0.02	13.73	7.41	
PMM 5884	2886.9180	3184.9180	3.03	0.02	8.83	6.21	
PMM 5884	3631.8528	3906.8528	3.04	0.02	8.76	6.75	
PMM 5884	4090.7318	4298.7318	3.03	0.02	6.93	4.15	
PMM 665	1868.8053	5137.8208	4.51	0.04	14.02	5.92	complete
PMM 665	1872.7631	2079.7631	4.6	0.8	7.09	6.15	
PMM 665	2168.8629	2257.7139	4.52	0.08	10.05	8.04	
PMM 665	3358.7697	3559.7697	4.51	0.04	6.11	6.07	
PMM 686	1868.8053	5137.8208	4.31	0.04	8.84	6.89	complete
PMM 686	4091.7565	4967.7565	4.14	0.03	6.57	6.27	
PMM 6974	1868.8053	5161.8371	7.8	0.5	30.77	7.59	complete
PMM 6974	2546.8298	2828.8298	7.8	0.1	8.17	5.27	
PMM 6974	2886.9180	3184.9180	7.7	0.1	10.45	8.62	
PMM 6974	3356.7807	3561.7807	7.7	0.1	13.82	5.02	
PMM 6974	4090.7318	4665.7318	7.8	0.1	8.44	8.13	
PMM 6978	1868.8144	5161.8371	5.1	0.2	41.75	7.25	complete
PMM 6978	2546.8298	2828.8298	5.10	0.05	5.92	5.92	
PMM 6978	3356.7807	3561.7807	5.13	0.05	17.04	7.42	
PMM 6978	4090.7318	4665.7318	5.11	0.05	18.53	8.05	
PMM 6978	4723.8939	5020.8939	5.12	0.05	6.87	6.04	
PMM 7422	1868.8046	5161.8149	1.512	0.005	17.62	10.49	complete
PMM 7422	2168.8629	2256.6919	1.504	0.009	10.41	5.48	
PMM 7422	2546.8298	2828.8298	1.512	0.005	15.04	5.78	
PMM 7422	2886.9180	3185.9180	1.512	0.005	40.56	5.50	
PMM 7422	3359.7666	3542.7666	1.512	0.005	16.94	5.15	
PMM 7422	3631.8853	3906.8853	1.512	0.005	18.19	6.17	
PMM 7422	4090.7318	4283.7318	1.461	0.004	6.26	4.71	
PMM 7422	4723.8939	4906.8939	1.524	0.005	7.51	6.32	
PMM 756	1868.8053	5137.8208	3.14	0.02	114.09	7.67	complete

Table B.2 (cont'd)

Target	JD Initial	JD Final	Period (d)	ΔP (d)	Normalised Power	Power at 99% Confidence Level	note
PMM 756	1872.7631	2079.7631	3.14	0.02	15.40	6.54	
PMM 756	2173.8772	2257.7139	3.15	0.04	17.48	5.29	
PMM 756	2546.8499	2828.8499	3.14	0.02	19.78	6.74	
PMM 756	2886.9180	3184.9180	3.15	0.02	19.47	6.02	
PMM 756	3358.7697	3559.7697	3.17	0.02	6.24	5.35	
PMM 756	3622.9120	3906.9120	3.14	0.02	22.12	7.41	
PMM 756	4091.7565	4967.7565	3.14	0.02	51.66	7.68	
PMM 7956	1868.8038	5161.8371	1.002	0.002	16.11	6.65	complete
PMM 8415	1868.8053	5129.8602	0.998	0.004	35.29	8.61	complete
TYC 7695 0335 1	1873.7725	2083.7725	0.3913	0.0003	8.13	7.42	
TYC 7695 0335 1	2168.8989	2251.7426	0.3913	0.0009	5.37	4.27	
TYC 7695 0335 1	3358.7893	3561.7893	0.3913	0.0003	5.59	4.98	
TYC 7695 0335	3863.2391	3906.2541	0.391	0.001	24.59	6.33	SW complete
TYC 7695 0335	4176.2594	4238.2750	0.391	0.0009	48.55	4.66	SW
TYC 7695 0335	4454.4332	4512.4332	0.391	0.0009	125.67	7.24	SW
TYC 7695 0335	4512.4332	4570.4332	0.391	0.0009	130.12	9.70	SW
TYC 8594 0058 1	1872.7631	2079.7631	0.982	0.002	11.11	6.87	
TYC 8594 0058 1	2172.8936	2248.7278	1.014	0.006	5.05	4.83	
TYC 8594 0058 1	2886.9180	3184.9180	0.982	0.002	5.25	4.99	
TYC 8594 0058 1	3622.9120	3906.9120	0.982	0.002	7.98	5.42	
TYC 9217 0641 1	1868.8180	5145.8394	2.30	0.01	45.36	9.24	complete
TYC 9217 0641 1	1873.8054	2102.8054	2.31	0.01	12.74	5.26	
TYC 9217 0641 1	2541.8851	2840.8851	2.30	0.01	17.02	5.36	
TYC 9217 0641 1	2900.8970	3187.8970	2.30	0.01	11.27	5.11	
TYC 9217 0641 1	3642.8878	3905.8878	2.31	0.01	20.46	7.08	
TYC 9217 0641 1	4090.7481	4305.7481	2.32	0.01	14.76	5.64	
TYC 9217 0641 1	4365.8814	5047.8814	2.31	0.01	18.95	7.13	

Table B.3 ϵ Cha association and η Cha cluster. Summary data from the literature and mass and radius derived from evolutionary tracks.

Name	RA (2000.0)	DEC (2000.0)	V (mag)	B−V (mag)	V−I (mag)	M_V (mag)	d (pc)	$v \sin i$ (km s^{-1})	Mass ($M_\odot$)	Radius ($R_\odot$)	Sp.T	MGR	n1
ϵ Chamaeleontis													
CP-68 1388	10 57 49.30	-69 14 00.00	10.04	0.86	0.93	4.79	112	25.90	1.1	1.60	K1V(e)	ϵ Cha	A/0 A_v
GSC 9419-01065	11 49 31.90	-78 51 01.00	11.90	1.27	1.80	8.31	52	18.00	0.7	1.00	M0Ve	ϵ Cha	A/0 A_v
HIP 58285	11 57 13.50	-79 21 32.00	10.19	0.93	0.88	6.09	66	39.00	0.9	0.90	K0e	ϵ Cha	A/2 A_v
HIP 58490	11 59 42.30	-76 01 26.00	10.65	1.02	1.11	5.80	93	10.20	1.0	1.25	K4Ve	ϵ Cha	A/0 A_v
HD 104237E	12 00 09.30	-78 11 42.00	10.28	1.11	1.11	4.95	116	30.00	1.1	1.40	K4Ve	ϵ Cha	T/2 A_v
HD 104467	12 01 39.10	-78 59 17.00	8.32	0.63	0.68	3.23	104	22.20	1.1	1.80	G3V(e)	ϵ Cha	A/0 A_v
GSC 9420-0948	12 02 03.80	-78 53 01.00	11.02	1.00	1.40	5.62	120	12.00	1.1	1.60	K7e	ϵ Cha	A/1 A_v
GSC 9416-1029	12 04 36.20	-77 31 35.00	13.16	1.30	2.16	7.71	123	6.00	0.7	1.40	M2e	ϵ Cha	A/1 A_v
HD 105923	12 11 38.10	-71 10 36.00	8.97	0.73	0.80	3.66	115	13.10	1.1	1.80	G8V	ϵ Cha	A/0 A_v
GSC 9239-1495	12 19 43.50	-74 03 57.00	12.06	1.28	1.80	6.95	105	...	1.0	1.40	M0e	ϵ Cha	A/1 A_v
GSC 9239-1572	12 20 21.90	-74 07 39.00	11.50	0.97	1.40	6.29	110	41.00	1.0	1.30	K7Ve	ϵ Cha	A/1 A_v
GSC 9235-1702	12 21 04.99	-71 16 49.27	11.62	1.20	1.60	7.80	58	...	0.8	0.90	K7V	ϵ Cha	A/2
CD-74 712	12 39 21.20	-75 02 39.00	10.22	0.97	1.08	5.16	103	20.20	1.0	1.50	K3Ve	ϵ Cha	A/0
CD-69 1055	12 58 25.60	-70 28 49.00	9.57	0.83	0.88	4.54	101	24.30	1.1	1.40	K0Ve	ϵ Cha	A/0 A_v
TYC 9246 971 1	13 22 7.60	-69 38 12.00	9.95	0.86	0.93	4.88	103	14.20	1.1	1.40	K1Ve	ϵ Cha	A/0 A_v

A: V mag from ASAS; T: V mag from Torres et al. (2006); 0: V−I from Torres et al. (2006); 1: V−I from Alcalà et al. (1995); 2: V−I from Sp. Type; A_v: corrected for extinction.

η Chamaeleontis													
RECX1	08 36 56.2	-78 56 46.0	10.36	1.19	1.39	5.41	97.3	21.70	1.0	1.80	K4Ve	η Cha	A/0
RECX3	08 41 37.2	-79 03 30.9	14.30	...	2.45	9.35	97.3	10.50	0.3	1.00	M3	η Cha	A/0
RECX4	08 42 23.7	-79 04 03.6	12.73	...	1.92	7.78	97.3	5.96	0.8	1.00	K7	η Cha	A/0
RECX5	08 42 27.3	-78 57 48.5	15.17	...	2.80	10.22	97.3	8.75	0.2	1.00	M5	η Cha	A/0
RECX6	08 42 39.0	-78 54 43.5	13.98	...	2.35	9.03	97.3	20.9	0.4	1.00	M2	η Cha	A/0
RECX7	08 43 07.7	-79 04 52.3	10.76	...	1.36	5.81	97.3	32	1.1	1.60	K3	η Cha	A/0
RECX9	08 44 16.6	-78 59 08.9	14.75	...	2.87	9.80	97.3	...	0.3	1.20	M4	η Cha	A/0
RECX10	08 44 32.2	-78 46 31.7	12.41	...	1.77	7.46	97.3	<5	0.9	1.20	K7	η Cha	A/0
RECX11	08 47 01.8	-78 59 35.2	11.00	...	1.36	6.05	97.3	13	1.0	1.20	K4	η Cha	A/0
RECX12	08 47 56.9	-78 54 54.0	13.92	0.73	2.34	8.97	97.3	15.00	0.4	1.00	M3e	η Cha	A/0
RECX14	08 41 30.6	-78 53 07.0	17.07	...	3.25	12.12	97.3	...	0.1	0.80	M4	η Cha	L/0
RECX15	08 43 18.4	-79 05 21.0	13.97	...	2.20	9.02	97.3	...	0.5	0.90	M2	η Cha	A/0
RECX16	08 44 09.1	-78 33 46.0	17.07	...	4.0	12.12	97.3	...	...	...	M5e	η Cha	L/1
RECX17	08 38 51.5	-79 16 14.0	16.82	...	4.0	11.89	97.3	...	...	...	M5e	η Cha	L/1
RECX18	08 36 10.6	-79 08 18.0	17.66	...	4.0	12.71	97.3	...	...	...	M5e	η Cha	L/1

A: V mag from ASAS; L: V mag from Lawson et al. (2002); 0: V−I from Lawson et al. (2001, 2002); 1: V−I from Sp. Type

Table B.4 Octans association. Summary data from the literature and mass and radius derived from evolutionary tracks.

Name	RA (2000.0)	DEC (2000.0)	V_{min} (mag)	B−V (mag)	V−I (mag)	M_V (mag)	d (pc)	$v \sin i$ (km s^{-1})	Mass ($M_\odot$)	Radius ($R_\odot$)	Sp.T	MGR	n1
CD-58 860	04 11 55.60	-58 01 47.00	9.92	0.68	0.75	5.35	82	20.10	1.0	1.00	G6V	Oct	A/0
CD-43 1451	04 30 27.30	-42 48 47.00	10.75	0.79	0.90	5.35	120	19.70	1.0	1.00	G9V(e)	Oct	A/0
CD-72 248	05 06 50.60	-72 21 12.00	10.70	0.82	0.94	4.92	143	190.00	1.1	1.40	K0IV	Oct	A/0
HD 274576	05 28 51.40	-46 28 18.00	10.48	0.66	0.77	5.16	116	21.10	1.0	1.00	G6V	Oct	A/0
CD-47 1999	05 43 32.10	-47 41 11.00	10.05	0.56	0.67	3.94	167	39.00	1.1	1.40	G0V(e)	Oct	A/0
TYC 7066 1037 1	05 58 11.80	-35 00 49.00	10.77	0.80	0.84	4.90	149	20.50	1.0	1.15	G9V	Oct	A/1 A_v
CD-66 395	06 25 12.40	-66 29 10.00	10.75	0.71	0.91	4.91	147	190.00	1.1	1.45	K0IV	Oct	A/1
TYC 9300 0529 1	18 49 45.10	-71 56 58.00	11.59	0.80	0.91	5.13	196	25.80	1.0	1.20	K0V	Oct	A/0
TYC 9300 0891 1	18 49 48.70	-71 57 10.00	11.43	0.77	0.90	5.21	175	9.00	1.0	1.05	K0V(e)	Oct	A/0
CP-79 1037	19 47 03.90	-78 57 43.00	11.18	0.75	0.86	5.11	164	28.70	1.0	1.10	G8V	Oct	A/0
CP-82 784	19 53 56.70	-82 40 42.00	10.81	0.85	0.96	4.90	152	39.00	1.1	1.40	K1V	Oct	A/1
CD-87 121	23 58 17.70	-86 26 24.00	9.94	0.74	0.88	4.51	122	33.80	1.1	1.40	G8V	Oct	A/1

A: V mag from ASAS; 0: V−I from Torres et al. (2006); 1: V−I from Sp. Type; A_v: corrected for extinction.

Table B.5 Argus association and IC 2391 cluster. Summary data from the literature and mass and radius derived from evolutionary tracks.

Name	RA (2000.0)	DEC (2000.0)	V_{min} (mag)	B−V (mag)	V−I (mag)	M_V (mag)	d (pc)	$v \sin i$ (km s^{-1})	Mass ($M_\odot$)	Radius ($R_\odot$)	Sp.T	MGR	n1	
Argus														
HD 5578	00 56 55.50	-51 52 32.00	9.62	0.99	1.04	6.84	36	29.3	0.8	0.90	K3Ve	Arg	T/0	
CD-49 1902	05 49 44.80	-49 18 26.00	11.30	0.69	0.78	5.68	133	55.0	1.0	1.00	G7V	Arg	A/0	
CD-56 1438	06 11 53.00	-56 19 05.00	11.11	0.66	0.88	6.08	101	130.0	0.9	1.00	K0V	Arg	T/1	
CD-28 3434	06 49 45.40	-28 59 17.00	10.38	0.75	0.82	5.19	109	...	1.0	1.00	G7V	Arg	T/1	
CD-42 2906	07 01 53.40	-42 27 56.00	10.50	0.84	0.88	5.59	96	11.3	1.0	1.00	K1V	Arg	A/1	
CD-48 2972	07 28 22.00	-49 08 38.00	9.78	0.80	0.84	5.13	85	52.0	1.0	1.20	G8V	Arg	A/1	
HD 61005	07 35 47.46	-32 12 14.04	8.19	0.75	0.80	5.48	35	8.2	0.9	0.84	G8V	Arg	A/0	
CD-48 3199	07 47 26.00	-49 02 51.00	10.40	0.65	0.73	5.51	95	24.7	1.0	1.00	G7V	Arg	A/1	
CD-43 3604	07 48 49.60	-43 27 06.00	10.88	0.92	1.11	6.39	79	40.0	0.9	0.90	K4Ve	Arg	T/1	
TYC 8561 0970 1	07 53 55.50	-57 10 07.00	11.00	0.83	0.88	5.38	133	5.6	1.0	1.10	K0V	Arg	A/1	A_v
CD-58 2194	08 39 11.60	-58 34 28.00	10.08	0.62	0.72	4.95	106	85.0	1.0	1.00	G5V	Arg	A/1	
CD-57 2315	08 50 08.10	-57 45 59.00	10.21	0.83	1.06	5.34	94	23.7	1.0	1.40	K3Ve	Arg	T/1	
TYC 8594 0058 1	09 02 03.90	-58 08 50.00	11.08	0.71	0.83	5.33	141	34.1	1.0	1.10	G8V	Arg	A/1	
CPD-62 1197	09 13 30.30	-62 59 09.00	10.46	0.81	0.93	5.23	111	84.0	1.0	1.20	K0V(e)	Arg	T/0	
TYC 7695 0335 1	09 28 54.10	-41 01 19.00	11.62	0.67	0.74	5.84	143	120.0	0.9	1.00	K3V	Arg	T/1	
HD 84075	09 36 17.80	-78 20 42.00	8.59	0.59	0.66	4.59	63	20.0	1.0	1.10	G1	Arg	A/0	
TYC 9217 0641 1	09 42 47.40	-72 39 50.00	12.18	0.65	0.93	6.58	132	23.4	0.8	0.90	K1V	Arg	A/1	
CD-39 5883	09 47 19.90	-40 03 10.00	10.74	0.81	0.88	5.74	100	10.8	0.9	1.00	K0V	Arg	A/1	
HD 85151A	09 48 43.30	-44 54 08.00	9.10	0.50	0.78	4.91	69	...	1.0	1.20	G7V	Arg	A/1	
CD-65 817	09 49 09.00	-65 40 21.00	10.33	0.63	0.69	4.58	141	19.2	1.0	1.10	G5V	Arg	T/0	
HD 309851	09 55 58.30	-67 21 22.00	9.78	0.60	0.68	4.72	103	19.8	1.0	1.20	G1V	Arg	A/0	
HD 310316	10 49 56.10	-69 51 22.00	10.82	0.73	0.78	5.28	128	16.3	1.0	1.00	G8V	Arg	T/0	
CP-69 1432	10 53 51.50	-70 02 16.00	10.66	0.62	0.71	4.59	164	55.0	1.0	1.20	G2V	Arg	T/0	
CD-74 673	12 20 34.40	-75 39 29.00	10.28	1.02	1.06	6.78	50	12.0	0.8	0.90	K3Ve	Arg	A/1	
CD-75 652	13 49 12.90	-75 49 48.00	9.61	0.68	0.76	5.07	81	20.1	1.0	1.10	G1V	Arg	A/0	
HD 133813	15 12 23.40	-75 15 15.00	9.27	0.84	0.86	5.78	50	10.8	0.9	1.00	G9V	Arg	A/0	
CD-52 9381	20 07 23.80	-51 47 27.00	10.01	1.24	1.25	7.70	29	42.0	0.7	0.80	K6Ve	Arg	A/1	

A: V mag from ASAS; T: V mag from Torres et al. (2006); 0: B−V and V−I from Torres et al. (2006);
1: B−V from Torres et al. (2006) and V−I from Sp.Type; A_v: corrected for extinction.

IC 2391														
PMM 7422	8 28 45.67	-52 05 26.70	10.40	0.69	0.75	5.00	120	33.0	1.0	1.00	G6	Arg	A/1	
PMM 7956	8 29 51.90	-51 40 40.00	11.50	0.97	1.06	5.75	141	14.0	1.0	1.00	Ke	Arg	A/1	
PMM 1560	8 29 52.40	-53 22 00.00	10.64	0.61	0.72	4.99	135	6.0	1.0	1.00	G3	Arg	P/1	
PMM 6974	8 34 18.10	-52 15 58.00	12.04	1.04	1.17	6.20	147	5.0	0.9	1.00	...	Arg	A/1	
PMM 4280	8 34 20.50	-52 50 05.00	10.04	0.67	0.74	4.20	145	16.0	1.0	1.60	G5	Arg	P/1	
PMM 6978	8 35 1.20	-52 14 01.00	12.01	1.02	1.14	6.47	128	7.0	0.9	0.90	...	Arg	P/1	
PMM 2456	8 35 43.70	-53 21 20.00	12.16	0.92	0.98	6.51	135	48.0	0.8	0.90	K3e	Arg	A/1	
PMM 351	8 36 24.20	-54 01 06.00	10.17	0.57	0.70	4.63	128	90.0	1.0	1.20	G0	Arg	P/1	
PMM 3359	8 36 55.00	-53 08 34.00	11.38	0.76	0.80	5.70	137	9.0	1.0	1.00	...	Arg	A/1	
PMM 5376	8 37 2.30	-52 46 59.00	13.94	1.37	1.73	8.33	132	10.0	0.7	0.80	Me	Arg	A/1	
PMM 665	8 37 51.60	-53 45 46.00	11.33	0.75	0.79	5.61	139	8.0	1.0	1.00	G8	Arg	P/1	
PMM 4336	8 37 55.60	-52 57 11.00	11.25	0.86	0.97	5.53	139	8.0	1.0	1.10	G9	Arg	A/0	
PMM 4362	8 38 22.90	-52 56 48.00	10.91	0.67	0.74	5.07	147	10.0	1.0	1.10	...	Arg	A/0	
PMM 4413	8 38 55.70	-52 57 52.00	10.20	0.67	0.74	4.45	141	9.0	1.0	1.40	G2	Arg	A/1	
PMM 686	8 39 22.60	-53 55 06.00	12.55	1.04	1.11	6.87	137	13.0	0.8	0.90	K4e	Arg	A/1	
PMM 4467	8 39 53.0	-52 57 57.00	11.80	0.86	0.91	6.11	137	7.0	0.9	1.00	K0(e)	Arg	A/1	
PMM 1083	8 40 6.20	-53 38 07.00	10.38	0.57	0.69	4.66	139	43.0	1.0	1.20	G0	Arg	A/0	
PMM 8415	8 40 16.30	-52 56 29.00	11.63	0.87	0.94	5.88	141	21.0	0.9	1.00	G9(e)	Arg	A/0	
PMM 1759	8 40 18.30	-53 30 29.00	11.62	1.01	1.06	5.96	135	4.0	0.9	1.00	K3e	Arg	A/0	A_v
PMM 1142	8 40 49.10	-53 37 45.00	11.04	0.68	0.80	5.20	147	8.0	1.0	1.00	G6	Arg	A/0	
PMM 1820	8 41 25.90	-53 22 41.00	12.41	1.00	1.23	6.47	154	89.0	0.9	1.00	K3e	Arg	A/0	
PMM 4636	8 41 57.80	-52 52 14.00	13.20	1.26	1.55	7.55	135	5.0	0.8	0.90	K7e	Arg	A/0	
PMM 3695	8 42 18.60	-53 01 57.00	13.30	1.44	2.07	7.62	137	90.0	0.8	1.40	M2e	Arg	A/0	
PMM 756	8 43 0.40	-53 54 08.00	11.06	0.68	0.74	5.19	149	16.0	1.0	1.00	G9	Arg	A/1	
PMM 2012	8 43 59.00	-53 33 44.00	11.41	0.83	0.90	5.76	135	19.0	0.9	1.00	K0(e)	Arg	A/0	
PMM 4809	8 44 5.20	-52 53 17.00	10.73	0.64	0.75	4.79	154	16.0	1.0	1.10	G3(e)	Arg	A/0	
PMM 1373	8 44 10.20	-53 43 34.00	12.06	0.96	1.04	6.31	141	7.0	0.9	0.90	...	Arg	A/1	
PMM 5884	8 44 26.20	-52 42 32.00	11.35	0.73	0.84	5.63	139	13.0	1.0	1.00	G9(e)	Arg	A/0	
PMM 4902	8 45 26.90	-52 52 02.00	12.45	1.05	1.24	6.83	133	7.0	0.8	0.90	K3e	Arg	A/0	
PMM 2182	8 45 48.00	-53 25 51.00	10.18	0.63	0.66	4.27	152	78.0	1.0	1.40	G2(e)	Arg	A/1	

A: V mag from ASAS; P: V mag from Platais et al. (2007); 0: B−V and V−I from Patten & Simon (1996);
1: B−V from Platais et al. (2007) and V−I from Sp. Type; A_v: corrected for extinction.